



UNIVERSITÀ POLITECNICA DELLE MARCHE  
Repository ISTITUZIONALE

How urban layout and pedestrian evacuation behaviours can influence flood risk assessment in riverine historic built environments

This is the peer reviewed version of the following article:

*Original*

How urban layout and pedestrian evacuation behaviours can influence flood risk assessment in riverine historic built environments / Bernardini, Gabriele; Romano, Guido; Soldini, Luciano; Quagliarini, Enrico. - In: SUSTAINABLE CITIES AND SOCIETY. - ISSN 2210-6707. - ELETTRONICO. - 70:(2021). [10.1016/j.scs.2021.102876]

*Availability:*

This version is available at: 11566/291492 since: 2024-04-23T07:35:01Z

*Publisher:*

*Published*

DOI:10.1016/j.scs.2021.102876

*Terms of use:*

The terms and conditions for the reuse of this version of the manuscript are specified in the publishing policy. The use of copyrighted works requires the consent of the rights' holder (author or publisher). Works made available under a Creative Commons license or a Publisher's custom-made license can be used according to the terms and conditions contained therein. See editor's website for further information and terms and conditions.

This item was downloaded from IRIS Università Politecnica delle Marche (<https://iris.univpm.it>). When citing, please refer to the published version.

(Article begins on next page)

**POSTPRINT OF Bernardini G, Romano G, Soldini L, Quagliarini E (2021) How urban layout and pedestrian evacuation behaviours can influence flood risk assessment in riverine historic built environments. Sustainable Cities and Society 70:102876. <https://doi.org/10.1016/j.scs.2021.102876>**

---

- Flood emergency in Historic Built Environments (HBEs) is investigated.
- **Typical HBEs** are defined on case-studies data classification.
- Hydrodynamics and pedestrian evacuation simulations are performed on them.
- Results are organized in risk indexes **with and without** pedestrian evacuation behaviors.
- Risk differences **with and without** pedestrian evacuation behaviors are noticed in each outdoor space in the HBE.

# How urban layout and pedestrian evacuation behaviours can influence flood risk assessment in riverine historic built environments

## Abstract

Riverine Historic Built Environments (HBEs) in urban centres are relevant scenarios for flood risk, due to the compact layout of their outdoor spaces, that are squares and streets, and their position in flood-prone areas. Differences in HBE layout can provide differences in flood risks, but excluding the response of exposed individuals can lead to risk underestimation or overestimation, as for other hazards. This work is a first attempt to compare how accounting or not pedestrian evacuation behaviours can affect flood risk assessment and emergency strategies evaluation. Parametric configurations of typical HBEs are provided on case-studies, and existing tools for hydrodynamic and pedestrian evacuation simulation are applied to them. Risk indexes for the whole HBE (macroscale) and each of its outdoor space (microscale) in it are provided. Results show how the risk indexes trends accounting or not pedestrian evacuation behaviours at the macroscale are similar, while differences at the microscale exist (about 15% in absolute terms). Concerning emergency strategies, sheltering seems to decrease the risk for the whole HBE up to 33% in comparison to leaving the flood-affected area. Results also support where/how to place gathering areas in the HBE.

**Keywords:** flood; evacuation simulation; risk assessment; simulator; risk index; historic built environment; emergency management

## 1. Introduction

In the last decades, floods have been the most common and devastating natural hazard causing disasters for our cities and their society (Gu, 2019; Young & Jorge Papini, 2020), affecting more individuals and emergency management authorities worldwide than any other hazard (European Commission, 2017).

Risks and effects of floods in the built environment of our cities are increasing because of severity-affecting factors, such as the densification of urban areas, urbanization growth and changes in land use (Nguyen et al., 2019; Young & Jorge Papini, 2020). Thus, the society in urban areas will be more and more vulnerable to flood consequences, because of the gradual shift in population residence from rural to urban areas, which is estimated to pass from 55% to 68% in 2050 (United Nations, 2018), as well as of the impacts of climate change on the occurrence of floods (European Commission, 2017; Gu, 2019).

In this context, riverine Historic Built Environments (HBEs) are generally characterized by a high flood impact, because of the combination between different factors (Arrighi et al., 2013; Ferreira & Santos, 2020; La Rosa & Pappalardo, 2020; Lanza, 2003; Ortiz et al., 2016; Rezende, Miranda, et al., 2019; Wang, 2015), such as: (1) the position in flood-prone areas; (2) their compact HBE layout considering its outdoor spaces, that are

squares and streets; (3) the significant building heritage vulnerability; (4) the high population density and the consistent presence of visitors, who can be unaware of the risk and unfamiliar with the HBE layout; (5) the possible inefficient early warning systems; (6) the limitations to defensive infrastructural measures in artificial drainage and sewer systems, as well as their possible related failures over the time.

As for other kinds of disasters such as earthquakes, fire and terrorist acts (Bernardini et al., 2019; Kobes et al., 2010; Lin et al., 2020) and according to the general definition on disaster risk reduction<sup>1</sup>, flood risk assessment depends on the combination of three main classes of factors (Arrighi et al., 2013; Balica et al., 2013; Bernardini, Camilli, et al., 2017; Ferreira & Santos, 2020; Lumbroso & Davison, 2018; Villagràn De León, 2006):

1. the *vulnerability* of the HBE, and, in particular, the *physical vulnerability*-related factors increasing the susceptibility to the impacts of flood hazard of the individuals hosted in the HBE;
2. the *flood hazard*, that includes the characteristics of the phenomenon causing damage in the HBE;
3. the *exposure* by considering at least the number of exposed individuals, to be combined with their capacity to face the disaster, which relies on *pedestrian evacuation behaviours* and the adopted emergency management strategies.

However, most of the current approaches generally only take into account *physical vulnerability* and *hazard* evaluations (Arrighi et al., 2013; Ferreira & Santos, 2020; Ortiz et al., 2016) or just combine such factors with the number and location of exposed individuals (La Rosa & Pappalardo, 2020).

Besides, existing approaches generally provide macroscale results to suggest risk-mitigation strategies concerning the best position of gathering areas in wide urban scenarios and the modification to the emergency path configurations in respect to the layout (Lumbroso & Davison, 2018; Shirvani et al., 2020; Zhuo & Han, 2020). At the same time, contrarily to other kinds of disasters affecting the urban layout such as earthquakes (Zlateski et al., 2020), the microscale analysis of the outdoor space affecting the pedestrians' safety seems to be generally neglected (Bernardini, Postacchini, et al., 2017).

Furthermore, a very limited number of researches try to include *pedestrian evacuation behaviours* (Lumbroso

---

<sup>1</sup> <https://www.undrr.org/terminology>, last access: 10/12/2020

& Davison, 2018; Melo et al., 2020), while no work directly deals with the particular but widespread context of riverine HBEs and differences in risk evaluations with and without evacuation behaviours.

In this context, this work wants to start filling this gap by comparing how accounting or not the *pedestrian evacuation behaviours* can affect the flood risk assessment and the definition of risk mitigation strategies in HBEs. To this end, a novel simulation-based methodology is proposed taking advantages of a parametric description of the HBE itself.

Risk indexes are proposed to assess the risk with and without the *pedestrian evacuation behaviours*, by innovatively adopting the two scales of application in a combined manner. The macroscale analysis, concerning the HBE as a whole, can globally compare and rank different HBEs and emergency management strategies. The microscale analysis, concerning each outdoor space (street, square, or a part of them) composing the HBE, can provide data on where and how to introduce interventions for supporting the pedestrians' evacuation in each typical HBE.

Sustainability criteria are pursued in relation to:

1. the methodology, by preferring easy-to-use simulation and assessment tools which can be quickly employed also by low-trained technicians and non-expert stakeholders;
2. the risk-management solutions, by assessing the better emergency management strategies for each HBE scenario in terms of intervention efforts, also in respect to the heritage to be preserved. In particular, solutions are aimed at facing different emergency scenarios and directly supporting pedestrians in evacuation conditions through physical devices, such as handrails or raised platform (to be applied where they are needed, depending on the *pedestrian evacuation behaviours*).

In the following, *physical vulnerability* (Section 1.1), *hazard* (Section 1.2), *exposure* and *pedestrian evacuation behaviours* (Section 1.3) characterising HBEs are briefly discussed as the pillars of the proposed approach.

### 1.1. Physical vulnerability

The urban layout is a prominent issue in the *physical vulnerability* of the HBE (Ferreira & Santos, 2020; La Rosa & Pappalardo, 2020; Soares-Frazão & Zech, 2008). In fact, the morphological configuration of outdoor spaces and their composing materials, such as the permeability of the surfaces, affect the floodwaters

spreading, in terms of speed  $V$  [m/s] and depth  $D$  [m], according to open-channel related effects (Ferreira & Santos, 2020; La Rosa & Pappalardo, 2020; Soares-Frazão & Zech, 2008). Several experimental-based studies performed under different idealized conditions (Beretta et al., 2018; Soares-Frazão & Zech, 2008; Testa et al., 2007; Velickovic et al., 2017) pointed out that the main layout features seem to be: aligned or staggered layout; buildings orientation in respect to the flow; ratio between the building sides length; building length/street width ratio.

## 1.2. Hazard

The floodwater spreading into the layout over time and space depends on the flooding type (European Commission, 2015). Among the flooding types, the fluvial flooding is one of the most relevant and recurrent (Ferreira & Santos, 2020; Mogollón et al., 2016; Wizer & Mpigi, 2020). According to international reports (European Commission, 2015), fluvial floods represent 66% of historical events and 76% of potential future events. They are mainly characterized by natural exceedance as flooding mechanism in 51% of historical events and 45% of potential future events, thus stressing the importance of considering severe conditions for flood safety assessment and risk-mitigation strategies.

Many existing hydrologic–hydraulic models can be applied to riverine scenarios for fluvial flood simulation and assessment (Arrighi et al., 2013). Shallow-water depth-averaged approaches (Arrighi et al., 2013; Bazin et al., 2017; Bernardini, Postacchini, et al., 2017; Soares-Frazão & Zech, 2008) seem to be promising ones because of: (1) the possibility to represent the complex interactions between water flows and street/building patterns; (2) the consistency with the spatial scale application of the HBE, combining an adequate level of detail (0.1m to 10m) and accuracy (especially in case of compact layout) with low computational costs.

In this context, one of the most powerful approaches seems to be represented by Nonlinear Shallow Water Equations-NSWE, which assumes that the floodwater motion on the vertical plane is negligible in respect to those on the horizontal plane.

## 1.3. Exposure and pedestrian evacuation behaviours

As for other kinds of emergencies such as cyclones, volcanic eruptions and earthquakes (Gu, 2019; Zlateski et al., 2020), the combination of *physical vulnerability* and *hazard* mainly affects the outdoor spaces during

the evacuation process because of (Arrighi et al., 2019; Bernardini, Camilli, et al., 2017; Chanson & Brown, 2015; Ferreira & Santos, 2020; Kontokosta & Malik, 2018; Kramer et al., 2016; La Rosa & Pappalardo, 2020; Melo et al., 2020; Oppen et al., 2010; Rezende, Guimarães, et al., 2019):

1. *the number of exposed individuals, and their features* such as age, gender, motion abilities;
2. *the individuals' reaction to the event and their evacuation behaviours*. Individuals can try to move in the outdoor spaces and gather in “safer” areas, thus interacting with the surrounding floodwaters. They are exposed to the majority of casualties during floods, due to the loss of body/vehicles stability, and are also slowed down depending on floodwater D and V;
3. *emergency and evacuation management procedures*, such as evacuation planning and rescuers' actions towards affected individuals. They are non-structural risk-reduction strategies and generally imply higher sustainability/adaptability since they can face different events by simple coordination actions. Related costs and efforts, including constant maintenance-related ones, are lower than those concerning permanent structural measures such as dikes, drainage/sewer system, and rivers restoration, which could also have a significant impact on the HBE features (e.g. layout, surfaces).

All these factors are considered in the *exposure* and *pedestrian evacuation behaviours* issues affecting the flood risk (Bernardini et al., 2019; Lombroso & Davison, 2018; Rezende, Miranda, et al., 2019; Shirvani et al., 2020). In fact, the evacuation process is fundamental when at least one of the following circumstances appears (Arrighi et al., 2019; Bernardini, Camilli, et al., 2017; Kolen & van Gelder, 2018; Lin et al., 2020; Melo et al., 2020; Wizer & Mpigi, 2020): (1) flash flood scenarios; (2) presence of pedestrians along the outdoor spaces (e.g. visitors); (3) possible difficulties in moving upstairs for individuals placed at the ground levels, for instance, because of no connections between the floors/building activities, or the relationship between the building heights and the floodwater depths; (4) lacks of the effectiveness in early warnings, thus retarding the possibility to coordinate the evacuation before critical floodwater conditions are seen in the HBE; (5) the position of *emergency gathering areas* in the urban layout, i.e. in terms of distance, possibility to be reached by vehicles (e.g. in compact and narrow HBE).

Evacuation strategies can mainly refer to leaving the flood-affected area and gather outside of it (in the

following, *leaving*) or *sheltering* inside the area itself (Arrighi et al., 2019; Bernardini, Camilli, et al., 2017; Cools et al., 2016; Kolen & van Gelder, 2018; Lumbroso & Davison, 2018; Melo et al., 2020; Wood et al., 2018). In particular, *sheltering* strategies are relevant when:

1. **motor** vehicle evacuation cannot be performed, thus forcing individuals and/or rescuers to move on foot;
2. **nearby** safe areas or evacuation paths are easily reachable.

In particular, pedestrians placed in outdoor spaces, public buildings and **buildings** with no upper floors or limited occupants' capacity can try reaching the nearest gathering area.

Efforts towards evacuation simulation should prefer bottom-up and microscopic approaches (Yuksel, 2018), in which each pedestrian has his/her own skills and behaviours (speed, direction, dimension, evacuation target) and interacts with the surrounding HBE conditions, including D and V. Such microscopic simulators should be able to describe peculiar pedestrian behaviours in flood evacuation, such as speed reduction and stability depending on D and V, as well as attraction towards gathering areas and unmovable obstacles (Bernardini et al., 2020; Bernardini, Camilli, et al., 2017; Chanson & Brown, 2015; Cox et al., 2010).

## 2. Phases, materials and methods

The work is divided in three main phases.

The first phase concerns the definition of typical HBEs in riverine contexts and their risk-affecting conditions according to the literature review in Section 1. Five case studies in the Italian context (Albenga (SV), Carrara (MS), Colorno (PR), Montevarchi (AR), Senigallia (AN)) are selected as significant riverine HBEs to identify the main *vulnerability* modelling inputs in typical HBEs. They are characterized by a non-complex orography (i.e. essentially flat), and by a maximum population of 60.000 inhabitants. **Meanwhile**, they were affected by meaningful flood events in the last decades (i.e. since 1960). Appendix A resumes the main data for each case study according to Section 2.1 criteria. Input parameters are firstly collected to model the HBE physical vulnerability (Section 2.1). The HBE hazard is assessed by considering the overflow of the river, which is a recurring threat in riverine contexts (Section 2.2). Finally, *exposure* and *pedestrian evacuation behaviours* are



respectively organized in terms of the number of pedestrians involved in the simulation, and their behaviours in the evacuation process depending on the adopted “leaving” or “sheltering” strategy (Section 2.3).

In the second phase, the tools and the related procedures for simulation of floodwater spreading and emergency evacuation are selected and applied to the typical HBEs (Section 2.4).

Finally, simulation results are organized into Key Performance Indicators (KPIs) and risk indexes with and without the evacuation process (Section 2.5).

## 2.1. Physical vulnerability modelling

The following parameters are collected by orthophotos/technical maps from local administrations, and by Google Earth Pro v. 7.3.2<sup>2</sup> sources (Beretta et al., 2018; Soares-Frazão & Zech, 2008; Testa et al., 2007; Velickovic et al., 2017):

- a. *streets direction in respect to the river* [°], being parallel (0°) or perpendicular (90°);
- b. *average streets width* [m], to represent them as open channels having a quasi-constant geometry<sup>2</sup>;
- c. *average streets slope* [%], as the ratio between the height difference (from the highest point to the lowest one) and the total street length, according to Google Earth Pro altimetric profiles. Positive slopes indicate that: for the parallel streets, upstream spaces are higher than downstream spaces; for perpendicular streets, the altitude increases as you move far from the riverside;
- d. *dimensions of building blocks areas*, which are considered as non-floodable areas, according to a conservative approach to the simulation of floodwater levels in outdoor spaces. They are assumed in a simplified manner as rectangular shapes with parallel base  $b$  [m] and perpendicular length  $l$  [m] in relation to the river. Building blocks can have a parallel ( $b/l \geq 1$ ) or perpendicular ( $b/l < 1$ ) trend considering the river;
- e. *identification of squares*, which can ideally behave like detention basins. They are classified in terms of: (1) area<sup>3</sup> [m<sup>2</sup>]; (2) position (square adjoining the river; one or more building blocks between the

---

<sup>2</sup> <https://www.google.com/earth/index.html> (data retrieved at: 01/10/2018)

<sup>3</sup> Porticos were considered permeable to the floodwater, since they are characterized by very large openings on the ground floors (Gandini et al., 2020).

river and the square) and distance of the square barycentre from the river<sup>4</sup> [m]; (3) number of streets linked to the square [-]; (4) direction of the major axis of the square considering the river [parallel or perpendicular].

A statistical-based approach is applied to these parameters to define typical HBEs according to a perfect perpendicular streets mesh including squared/rectangular paved squares (i.e. with impermeable surfaced) (Beretta et al., 2018; De Sousa et al., 2019; Soares-Frazão & Zech, 2008). In particular, for each parameter, the mode is considered as a reasonable reference value to describe the common experimental-based conditions. Then, the typical HBEs are organized by varying the square presence, positioning and dimension. In detail, the square dimension is considered as multiple of 1 standard building block, namely *module*.

## 2.2. Hazard modelling

The modelled flood hazard considers the overflow of the river placed in the HBE to investigate the flood effect on the outdoor spaces and its users (European Commission, 2015; Ferreira & Santos, 2020).

Due to the lack of measured flood hydrograph and river cross-sections in the selected case studies, data from Esino River (Marche, Italy) are chosen for hazard modelling input definition. In detail, the hydrometer station located at Moie, placed in the central part of the Esino river basin, is selected because it registered frequent flood events since the 1960s. In fact, the Esino river is similar to the rivers of the case studies, both in terms of general basin features and maximum river section width [m] in the HBE if compared to the one of the Moie station (VV.AA., 2005). The model considers the overflow of the river placed in the HBE, in a short time span.

This condition implies that pedestrians could not reach safe areas before the event. The model is based on the Esino hydrograph related to the 18/11/1975 flood (VV.AA., 2005) and on the application of the theory of Giandotti (Giandotti, 1934) to the Esino River at the Moie section. Appendix B shows the calculation, which leads to a 100 years maximum flow rate of 1148 m<sup>3</sup>/s.

The following assumptions are taken into consideration to increase the effects of floodwater spreading in the outdoor spaces (Bernardini, Postacchini, et al., 2017; Chow, 1959; Soares-Frazão & Zech, 2008). *Building*

---

<sup>4</sup> The square near to the river in Albenga is excluded since it represents a specific condition referring to different aggregation in the HBE (parking areas linked to a crossroad junction nearby the main HBE area)

*blocks areas* are conservatively modelled as completely impermeable and with no surface roughness, thus inducing no dumping of floodwaters, no shear stress, and no speed reduction near to the buildings. The open channels bottom roughness is represented through the Manning's coefficient [ $s/m^{1/3}$ ] by considering a value equal to: (1) 0.030 for the riverbed, to model a natural stream having maximum width at floodstage lesser than 30m, non-vegetated and straight development; (2) 0.013 for the streets and squares, to model stone paving, which is typical of the considered Italian HBEs.

### 2.3. Exposure and pedestrian evacuation behaviours modelling

The number of pedestrians in outdoor spaces of the HBE is firstly defined to reproduce free-flow walking conditions for pedestrians placed along the streets before the flood. The threshold of pedestrians' densities  $\leq 5.6 \text{ m}^2/\text{pp}$  is adopted according to the Level of Service A threshold<sup>5</sup> (Bloomberg & Burden, 2006). 240 pedestrians are homogeneously positioned along the outdoor spaces in the HBE at the event peak time, to conservatively represent pedestrians, such as visitors, who cannot reach a building and move upstairs, according to Section 1.3 evacuation assumptions (Arrighi et al., 2019; Bernardini, Camilli, et al., 2017; La Rosa & Pappalardo, 2020).

Then, pedestrian evacuation behaviours in flood simulated in this work concern:

1. the pedestrian speed  $V_p$  [m/s] depending on the floodwater flow specific force for width unit  $M$  [ $\text{m}^3/\text{m}$ ] as in Eq. 1 (Bernardini, Camilli, et al., 2017):

$$V_p = 0.52 \cdot M^{-0.11}, \text{ where } M = \frac{V^2 \cdot D}{g} + \frac{D^2}{2} \quad \text{Eq. 1}$$

2. the limit conditions for stability in floodwaters depending on  $D$ ,  $V$  and the product between  $D$  and  $V$  ( $DV$ ) [ $\text{m}^2/\text{s}$ ] (Cox et al., 2010). In particular, the considered limits are  $DV \geq 1.20 \text{ m}^2/\text{s}$  or  $D \geq 1.20 \text{ m}$  or  $V \geq 3.0 \text{ m/s}$ , which refer to an adult;

3. pedestrians' attraction towards unmovable obstacles, such as walls and fences. Experimental data (Bernardini, Postacchini, et al., 2017) highlight that pedestrians generally try to maintain a distance from unmovable obstacles lower than 2.0m, or in any case lesser than 3.0m. The attractive trend further

<sup>5</sup> "Pedestrians move in desired paths without altering their movements in response to other pedestrians" (Bloomberg & Burden, 2006)

increases in the proximity of crossroads to speed up the crossing process;

4. the *choice of the evacuation target* depending on the considered emergency management strategy.

In the “*leaving*” strategy, the gathering areas are placed at the downstream exit of the HBE. In “*sheltering*” strategy, the gathering areas are placed in streets and squares where more favourable conditions in terms of  $D$ ,  $V$ ,  $DV$  occur. Thus, this value is derived from the hydrodynamic simulations, as pointed out in Section 2.2. The shortest path approach is adopted, and pedestrians cannot move upstream or towards the river, as in experimental-based behaviours (Bernardini, Postacchini, et al., 2017).

In this work, no differences due to the pedestrian features affecting speed, stability and evacuation path selection are considered, such as age, gender or motion abilities (Cox et al., 2010; Lumbroso & Davison, 2018). It is homogenously assumed that all the pedestrians are adults and are aware of the evacuation plan/gathering areas position, as well as no pre-movement phases exist.

#### 2.4. Simulation tools and procedures

A specific simulation setup is defined for each typical HBE layout derived from the *physical vulnerability* modelling in Section 2.1, for both the hydrodynamics and evacuation issues. Existing commercial software is selected to boost the application process and demonstrate the methodology capabilities also considering the use by local technicians in real HBE. Anyway, quick setup-based modifications to the evacuation simulator are provided to reproduce behaviours as in Section 2.3.

The floodwater spreading simulations are performed by Delft 3D (version 4.03.01<sup>6</sup>), because of reliable previous researches on its development, verification and application in urban contexts, including river overflow scenarios (Baky et al., 2020; Haq et al., 2020; Hassaballah et al., 2020; Sandbach et al., 2018). The software evaluates the effects of the fluvial flood on the outdoor spaces, by calculating  $D$  and  $V$  values<sup>7</sup> during the whole event, with time steps of 60s, on a solving mesh composed by 1m x 1m cells.

According to previous works criteria (Soares-Frazão & Zech, 2008), main gauging points are placed:

---

<sup>6</sup> Available: <https://oss.deltares.nl/web/delft3d> (downloaded at 01/12/2018)

<sup>7</sup>  $V$  is averaged on the  $D$ .

1. at each crossroad barycentre;
2. at each street barycentre;
3. in different points of each square by using a chessboard-based scheme according to Figure 1, to verify the possible effects due to floodwaters coming from the linked streets.

Figure 1 shows an example of the division of squares into 4 sub-spaces for each *module* by evidencing the river axis, the buildings (grey areas), the position of the gauging points inside the square (blue dots), the sub-spaces division (given by the dashed lines in the square). Each sub-space (dashed yellow area) is characterized by: (1) the Euclidean distance from the river axis  $d_r$  [m]; (2) 5 gauging points placed according to a chessboard scheme, and having a related distance depending on the length of the square axes.

$D$  and  $V$  from each gauging point are analysed to point out if general homogeneous conditions of floodwater spreading in the sub-space exist over time, by verifying that variations in measured  $DV$  are  $\leq 10\%$ . If the square dimension is equal to 2 building blocks areas, the scheme is repeated for each *module*.

In view of the above, for each outdoor space or each sub-space, namely  $i$ , output data concern the following issues:

1.  $D_i$  and  $V_i$ , which respectively are the maximum values of  $D$ ,  $V$ , are used to calculate the *pedestrian speed*  $Vp_i$ , while the *maximum value of  $DV_i$  during the simulation time*, namely  $DV_{max,i}$  [ $m^2/s$ ], is used to evaluate stability issues. The maximum values of the gauging point/points in the outdoor space/subspace during the simulation time are chosen to conservatively describe the floodwater effects on the pedestrian motion;
2. the Euclidean distance between the river axis and the *barycentre* of the outdoor space or sub-space, namely  $d_r$  [m], is used in risk assessment evaluation (see Section 2.5.1).

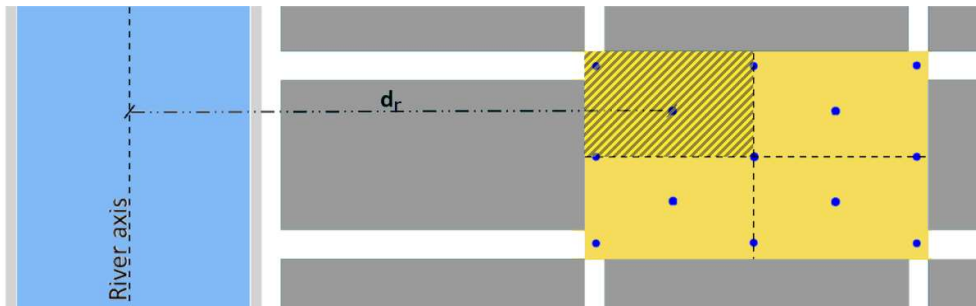


Figure 1: scheme of hazard analysis in a simulated square (example dimension equal to 1 module, by the yellow area), including gauging points positions (blue dots) and sub-spaces areas (divided by the dashed lines).

Evacuation simulations are performed by considering an overall simulation time  $t_{sim}$  [s] of 20 minutes (1200s).

$t_{sim}$  is centred on the simulation time at which the  $DV$  maximization is measured for the majority of outdoor spaces in the HBE. This time span is the greatest one ensuring that  $Vp_i$  and  $DV_i$  variations are generally  $\leq 10\%$ , by considering the streets and squares into the HBE. This threshold allows considering **simplified** quasi-constant environmental conditions affecting pedestrian motion (Bernardini, Postacchini, et al., 2017). Moreover, in view of the general timeline for flood emergency management (Oppen et al., 2010), the simulation time is compliant with previous works on evacuation simulations in the urban environment focusing on the evacuation process (Bernardini, Postacchini, et al., 2017).

These conditions are then implemented within the commercial Oasys MassMotion evacuation simulator (version 9.5<sup>8</sup>) (MassMotion Guide, 2017). Specific software setup is introduced to replicate the *pedestrian evacuation behaviours* considered in Section 2.3, without source-code modifications (see the supplementary data). In particular, the setup concerned the following points:

- the pedestrian speed depends on the  $D$  and  $V$  conditions **where** he/she is placed, according to  $Vp_i$  values in Equation 1;
- pedestrians placed **where**  $DV_i \geq 1.2 \text{ m}^2/\text{s}$  are considered as unable to arrive at a gathering area, thus being trapped in the outdoor spaces;
- pedestrians move along “preferential lanes”<sup>9</sup> placed 1m and 2m far from to the building walls, to replicate attraction towards unmovable obstacles. Simulation interactions between the pedestrians along these “preferential lanes” could provide variations of distance values between the pedestrian and the unmovable obstacles, thanks to pedestrian-pedestrian repulsive phenomena in motion;
- gathering areas are the evacuation destination and they are placed according to “leaving” and “sheltering” strategies. In *sheltering* strategy, they are placed in outdoor spaces where  $DV_i$  risk is low

<sup>8</sup> Available: <https://www.oasys-software.com/products/pedestrian-simulation/massmotion/> (downloaded at: 11/02/2019)

<sup>9</sup> “server” objects, characterized by “a conceptual entry point”, “an exit point” and a connecting line along which the simulated **pedestrians** can move according to queuing-based criteria to maintain their overall trajectory.

( $DV_i < 0.6 \text{ m}^2/\text{s}$ ). In this sense, analyses based on the  $DV$  conditions in the 1m x 1m grid can be performed to evaluate their effective position in the HBE layout and how they can be implemented (e.g. are raised platforms needed?).

## 2.5. Simulation results analysis for HBE risk assessment

Simulation results are organized into the KPIs concerning the *physical vulnerability* and the *hazard* modelling, as shown by Section 2.5.1, and the evacuation simulations, as shown by Section 2.5.2. Finally, KPIs are organized into risk indexes **with and without** considering *pedestrian evacuation behaviours*, as shown by Section 2.5.3.

**Both** KPIs and risk indexes are arranged by distinguishing the conditions of:

1. the overall HBE, according to a macroscale standpoint, thus providing a unique value for each typical HBE, expressed by the indexes subscript  $M$ ;
2. each outdoor space in the HBE, according to a microscale standpoint, thus providing, for each typical HBE, a specific value for each outdoor space, expressed by the indexes subscript  $m$ . In addition, a map view is offered to graphically trace the risk values on the HBE layout.

**All the KPIs** and the risk indexes are designed to range from 0 (no impact on risk) to 1 (maximum impact).

### 2.5.1. KPIs based on physical vulnerability and flood hazard

Table 1 resumes the KPIs concerning physical vulnerability and flood hazard, in view of the floodwater spreading simulation results.

First, **the microscale point of view is assumed to distinguish** each outdoor space and sub-space. **Thus**,  $DV_i$  maps over the HBE layout are traced according to Section 2.4 outputs.  $DV_i$  maps investigate the role of intrinsic features for streets and squares in the floodwater spreading in the typical HBEs scenarios.  $DV_i$  are organized into five risk classes considering the related conditions for adults' stability (Cox et al., 2010): safe, that is a null risk, if  $DV_i$  equal to  $0.0 \text{ m}^2/\text{s}$ ; low if up to  $0.6 \text{ m}^2/\text{s}$ ; moderate when ranging from  $0.6$  to  $0.8 \text{ m}^2/\text{s}$ ; significant when ranging from  $0.8$  to  $1.2 \text{ m}^2/\text{s}$ ; extreme if over  $1.2 \text{ m}^2/\text{s}$ .

Then, **the macroscale standpoint is investigated through** the *average DV value weighted by the outdoor spaces areas*  $DV_{a,M}$  [ $\text{m}^2/\text{s}$ ], **which considers** all the  $DV_i$  values of the outdoor spaces and sub-spaces in the

HBE.  $DV_{a,M}$  is normalized by the upper limit of stability (1.20 m<sup>2</sup>/s) to provide the *stability index for the whole HBE*  $I_{DV,M}$  [-]. Thus,  $I_{DV,M}$  can compare different scenarios. This work assumes  $I_{DV,M} = 1$  in case of  $DV_{a,M} > 1.20$  m<sup>2</sup>/s to stress similar unacceptable conditions for stability.

In a similar manner, the *stability index for each outdoor space*  $I_{DV,m}$  [-] depends on the ratio between  $DV_{max,i}$  [m<sup>2</sup>/s] and the critical threshold for adults' stability (1.20m<sup>2</sup>/s), thus analysing risks from a microscale standpoint. In addition, the *normalized distance of the outdoor space from the river*  $D_{r,m}$  [-] takes into account the distance-related effects from the flood source. It depends on  $d_{r,MAX}$  [m], which is the maximum  $d_r$  value in the HBE. Thus,  $D_{r,m}$  ranges from 0 to 1.

KPIs name, symbol [unit of measure]	KPIs calculation method	Evaluation of results
Average DV value weighted by the outdoor space areas, $DV_{a,M}$ [m <sup>2</sup> /s]	$DV_{a,M} = \frac{\sum DV_i A_i}{\sum A_i}$ [Eq. 2]	The higher is $DV_{a,M}$ , the more critical the overall HBE conditions for stability
Stability index for the HBE $I_{DV,M}$ and for each outdoor space $I_{DV,m}$ [-]	$I_{DV,M} = \min\left(\frac{DV_{a,M}}{1.20 \text{ m}^2/\text{s}}, 1\right)$ [Eq. 3]	The higher this index, the more probable is the loss of body stability (maximum value equal to 1)
	$I_{DV,m} = \min\left(\frac{DV_{max,i}}{1.20 \text{ m}^2/\text{s}}, 1\right)$ [Eq. 4]	
Normalized distance from the outdoor space to the river $D_{r,m}$ [-]	$D_{r,m} = 1 - \frac{d_r}{d_{r,MAX}}$ [Eq. 5]	The higher $D_{r,m}$ , the more rapid the arrival of the flood because of the shortest distance from the river

Table 1: KPIs for the macroscale and microscale risk-assessment concerning physical vulnerability and hazard.

### 2.5.2. KPIs based on pedestrian evacuation behaviours

Evacuation simulation results are organized into the macroscale-related KPIs described in Table 2. These KPIs trace the effects of interactions between pedestrians and floodwaters, depending on the adopted emergency evacuation strategy.

Considering the whole number of simulated pedestrians  $P$  [pp] (equal to 240 persons, according to Section 2.3), the following values are assessed for each scenario: (1) the maximum evacuation time  $t_{max,evac}$  [s], that is the one of the last pedestrian arriving at a gathering area; (2) the longest evacuation path  $d_{max}$  [m]; and (3) the number of pedestrians unable to arrive in a gathering area  $n_a$  [pp].

Maximum values are considered according to a conservative approach in simulation evaluation, since they offer different evacuation-related issues depending on the DV conditions in the outdoor spaces (Bernardini, Postacchini, et al., 2017).

If at least 1 pedestrian has to stop because of DV conditions,  $t_{max,evac}$  is conservatively assumed as the overall



simulation time  $t_{sim}$  [s], that is 1200s (20 minutes). The pedestrian flow at the gathering areas  $f_{e95}$  [pp/s] is calculated considering the 5<sup>th</sup> to 95<sup>th</sup> percentiles of pedestrians who can reach a gathering area. By this way, it is possible to exclude effects due to pedestrians who are: (1) initially placed in a particularly favourable position, such as close to the gathering areas, by referring to the 5<sup>th</sup> percentile as a threshold; or (2) involved in critical conditions for the evacuation flows, such as queuing phenomena, by referring to the 95<sup>th</sup> percentile as a threshold. The maximum value  $f_{e95,MAX}$  [pp/s] for all the compared HBE scenarios is also used as pointed out in Table 2.

KPIs name, symbol [unit of measure]	KPIs calculation method	Evaluation of results
Normalized evacuation time, $T_{e,M}$ [-]	$T_{e,M} = \frac{t_{max,evac}}{t_{sim}}$ [Eq. 6]	Higher is $T_{e,M}$ , higher is the time a pedestrian is exposed to risk
Normalized travelled distance, $D_{t,M}$ [-]	$D_{t,M} = \frac{d_{max,i}}{d_{MAX}}$ [Eq. 7]	The higher $D_{t,M}$ , the higher the possibility for the pedestrian to face additional threats (e.g. DV condition, obstacles dragged by floodwaters)
Percentage of non-arrived pedestrians, $N_{a,M}$ [-]	$N_{a,M} = \frac{n_a}{P}$ [Eq. 8]	Higher $N_{a,M}$ values relate to higher risk
Presence of trapped pedestrians in a given outdoor space, $N_{a,m}$ [boolean]	$N_{a,m} = 1 \text{ if } \frac{n_a}{P} \geq 0.05, N_{a,m} = 0 \text{ elsewhere}$ [Eq. 9]	Higher $N_{a,m}$ values relate to higher risk due to loss of stability or latecomers in the given outdoor space
Normalized pedestrian flow, $F_{e,M}$ [-]	$F_{e,M} = 1 - \frac{f_{e95}}{f_{e95,MAX}}$ [Eq. 10]	“Slower” evacuations are characterized by “lower” $f_{e95}$ values. Thus, higher $F_{e,M}$ values represent higher risk, since pedestrians take longer to reach shelter

Table 2: KPIs for the macroscale and microscale risk-assessment concerning the pedestrian evacuation behaviours.

Finally, from a microscale analysis standpoint, the *presence of trapped pedestrians in a given outdoor space*, namely  $N_{a,m}$  [boolean], is evaluated.  $N_{a,m}=1$  is conservatively assumed if the percentage of trapped pedestrians in the outdoor spaces is equal or higher than the 5% of  $P$ , according to general criteria for fire safety and evacuation simulation assessment (British Standards Institution, 2004). In fact, this threshold considers the effective risk conditions of 95% of the pedestrians, thus limiting the effects of local conditions affecting latecomers’ motion such as the initial positions of pedestrians, or the uncertainties in pedestrian interactions in the simulation model (D’Orazio et al., 2015; Schadschneider et al., 2009). Elsewhere,  $N_{a,m}=0$ .

### 2.5.3. Risk Indexes with and without the evacuation process

Risk Indexes are calculated by excluding and including evacuation-related issues, both at the macroscale and

microscale levels, by combining the KPIs through the Analytic Hierarchy Process methodology (Saaty, 1980)<sup>10</sup>.

The Analytic Hierarchy Process allows assigning priorities to the KPIs, which are assumed as criteria, according to pairwise comparisons between them. Each KPI weight  $W_k$  [-] permits a distinct evaluation between the single criterion importance and its global impact on the overall risk rating. Finally, KPIs are combined through Eq. 11, that outlines a *generic Risk Index RI* through the normalization in respect to its maximum value, where  $p$  is the overall number of KPIs considered for the *RI* calculation.

Eq. 11 is based on the *RI* representation according to the Euclidean norm of a vector in a vector space of dimension equal to  $p$ , and has a field of existence included in the range [0, 1], where 0 is the minimum risk and 1 represents the maximum risk. A classification of *RI* values is also proposed as follows to perform comparisons:  $RI < 0.15$ ;  $0.15 \leq RI < 0.30$ ;  $0.30 \leq RI < 0.45$ ;  $0.45 \leq RI < 0.60$ ;  $0.60 \leq RI < 0.75$ ;  $RI \geq 0.75$ .

$$RI = \sqrt{\frac{\sum_{k=0}^p W_k^2 \cdot KPI_k^2}{\sum_{k=0}^p W_k^2 \cdot 1^2}} \quad \text{Eq. 11}$$

The *macroscale RI without pedestrian evacuation behaviours*  $RI_{HBE,M}$  [-] is equal to  $I_{DV,M}$ . The *microscale index*  $RI_{HBE,m}$  [-] considers  $I_{DV,m}$  and  $D_{r,m}$ , by reasonably assuming that both of them have the same priority, since they refer to HBE and flood-related conditions ( $W_k=0.5$ ).

The *RI with pedestrian evacuation behaviours* is founded on the KPIs defined in Table 3. In particular, for the *macroscale RI with pedestrian evacuation behaviours*  $RI_{evac,M}$  [-], it is assumed that:

1.  $I_{DV,M}$  and  $N_{a,M}$  are the most important indicators since they describe the effect of HBE condition on *pedestrian evacuation behaviours*. Hence, when focusing on data related to each pedestrian, the priority is given to the possibility to reach a gathering area rather than to the evacuation time and distance;
2.  $T_{e,M}$  and  $F_{e,M}$  are considered on the same level of importance being both time-dependent indicators, even if they represent different evacuation issues.

The three KPIs were considered on the same level of importance the *microscale RI with pedestrian evacuation behaviours*  $RI_{evac,m}$  [-].

---

<sup>10</sup> Analytic Hierarchy Process calculator available at : [https://bpmmsg.com/academic/ahp\\_calc.php](https://bpmmsg.com/academic/ahp_calc.php) (last access: 10/06/2020).

Table 3 resumes the weight calculation for  $RI_{evac,M}$  and  $RI_{evac,m}$ , having a Consistency Ratio  $CR$  under acceptability thresholds ( $CR_M=0.3\%<10\%$ ;  $CR_m=0\%<10\%$ ).

	macroscale RI					microscale RI		
KPI	$T_{e,M}$	$D_{t,M}$	$N_{o,M}$	$F_{e,M}$	$I_{DV,M}$	$D_{r,m}$	$N_{o,m}$	$I_{DV,m}$
$W_k$ [-]	0.076	0.148	0.380	0.076	0.320	0.333	0.333	0.333

Table 3: weights  $W_k$  for RI with pedestrian evacuation behaviours obtained via Analytic Hierarchy Process.

Finally, due to their existence field  $[0, 1]$ , the proposed risk indexes are used as comparing elements to point out:

- the differences of RI with and without pedestrian evacuation behaviours, from both macroscale and microscale standpoints, by discussing reasons for differences, also in relation to the outdoor spaces (using maps in the HBE layout);
- according to a “macroscale” point of view: a) for RI without pedestrian evacuation behaviours, differences of risk levels in different typical HBE scenarios; b) RI with pedestrian evacuation behaviours, how different emergency evacuation strategies can affect the pedestrians’ safety, by comparing “leaving” to “sheltering” strategies;
- according to a “microscale” point of view, to highlight the main outdoor spaces in the HBE where the risk is higher and risk-reduction interventions should be hence applied, by discussing differences due to RI with and without pedestrian evacuation behaviours.

### 3. Results

#### 3.1. Physical vulnerability modelling: typical HBEs

Table 4 resumes the values of the parameters on physical vulnerability assessed on the case studies according to the statistical analysis. Two groups of typical HBEs are derived according to an aligned layout configuration as represented in Figure 2: (1) the compact layout in Figure 2-A (namely, Scenario 1); (2) the 5 layouts including a square in Figure 2-B (namely, Scenarios 2). The two scenarios group have the same basic profile sections (ground elevation along parallel and perpendicular streets), which are shown in Figure 2-C. The full building heights are not considered since they do not affect the results in terms of floodwater spreading into the HBEs layout. Furthermore, the two scenarios groups are based on the streets characterization according to the mode values of Table 4. Table 5 resumes the differences between the typical HBEs in Scenarios 2 (A to

E), due to the square positions in terms of distance from the river, and of dimensions in terms of *modules*, that is multiples of building blocks areas).



Figure 2: Typical HBEs considered in this work: A) compact layout (namely Scenario 1); B) typical HBEs layouts including the square (namely, Scenarios 2), having the same basic profile section as for Scenario 1.; c) the basic profile section (ground elevation) according to section lines S1 and S2 in panel A (vertical exaggeration scale: 10x) and metric scale for plan view for all the panels. In each panel, the riverbed is represented between the two grey lines on the left, the arrow points out the riverflow direction, and the full-coloured grey areas are building blocks

	Parallel streets		Perpendicular streets		Building Blocks
Percentile	Section width [m]	Avg Slope [%]	Section width [m]	Avg Slope [%]	b/l ratio [-]
25 <sup>th</sup>	4.0	0.3	5.1	-1.5	0.6
50 <sup>th</sup>	6.0	0.8	6.8	0.0	1.2
75 <sup>th</sup>	9.1	1.7	9.0	2.5	2.3
Mode	4.0	0.3	6.0	-0.6	0.5 (b = 33.0 m; l = 67.0 m)

Table 4: results from statistical analyses of case studies to define base features of the base typical HBE as in Figure 2-A (Scenario 1).

Case	Area [m <sup>2</sup> ]; [number of modules]	Distance from the river [m]	Number of streets linked [-]	Major axis of the square direction
A	2211; 1	100-150	8	Perpendicular
B	2211; 1	150-200	8	Perpendicular
C	2211; 1	0-100	8	Perpendicular
D	4554; 2	150-200	10	Perpendicular
E	4824; 2	100-150	10	Parallel

Table 5: description of Scenarios 2 as in Figure 2-B, by defining the square characterization. Assumed mode parameters for the HBE are the same of Table 4.

### 3.2. Hazard modelling: DV levels in outdoor spaces

The risk without the *pedestrian evacuation behaviours* combines the effects of the fluvial flood hazard and the *physical vulnerability* of *Scenarios 1* and *2*, by means of the analysis of *DV* levels in outdoor spaces. According to the hydrodynamic simulation results, regardless of the specific HBE scenario, critical *DV* conditions for each gauging point have been generally reached at about 45 minutes after the beginning of the flooding event. Figure 3 shows a representative example of this *DV* trend over time, referring to *Scenario 1*, and by considering different gauging points along the central perpendicular street.  $t_{sim}$  is hence centred with respect to this simulation time span.

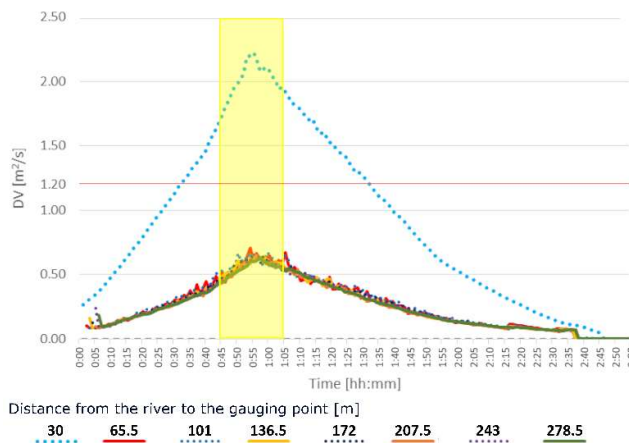


Figure 3: *DV* trend over time for *Scenario 1* by considering the central perpendicular street and for different distances [m] from the river. Straight lines refer to gauging points inside the outdoor spaces, dashed lines refer to those inside the crossroads. The yellow area highlights the time span for the simulations. The limit conditions for stability ( $DV=1.20\text{m}^2/\text{s}$ ) is also highlighted by the red continuous line.

Figure 4-A traces the overall  $DV_i$  maps for each of typical HBE. Such results firstly show that, in each typical HBEs, parallel streets have lower  $DV_i$  levels than the perpendicular ones. Therefore, low risk for stability exists, and higher  $V_{p_i}$  are allowed. The parallel street adjacent to the river has the highest risk levels in terms of  $DV_i$  because it is immediately and continuously affected by the river overflow.

Squares seem to additionally own the lowest  $DV_i$  values, being close to 0 in some sub-spaces of *Scenario 2.A* and *Scenario 2.B*. Nevertheless, *Scenario 2.C* shows significant differences because of its layout configuration in comparison to the others. The analysis of local maximum *DV* values at the solving mesh scale offers the reasons for such results, as shown by the example of Figure 4-B and by the overview of Figure C1 in Appendix C.

In particular, Figure 4-B shows these data for the square of *Scenario 2.E*, which are similar to those of

1  
2  
3  
4  
5  
6  
7  
8  
9  
10  
11  
12  
13  
14  
15  
16  
17  
18  
19  
20  
21  
22  
23  
24  
25  
26  
27  
28  
29  
30  
31  
32  
33  
34  
35  
36  
37  
38  
39  
40  
41  
42  
43  
44  
45  
46  
47  
48  
49  
50  
51  
52  
53  
54  
55  
56  
57  
58  
59  
60  
61  
62  
63  
64  
65

*Scenarios 2.A, 2.B and 2.D.* The upstream parts of the square, that is just near to the facing buildings, are characterized by  $DV$  close to  $0\text{m}^2/\text{s}$ , because the square generates a beneficial effect being like a detention basin and the facing buildings constrain waterflows from the streets placed upstream. On the contrary, the square in *Scenario 2.C* is placed close to the river and directly collects waters from river overflow, thus increasing the flows on the connected streets placed downstream. These streets should discharge higher floodwater flows but they have limited widths, and so their  $DV_i$  values are sensibly higher than in all the other typical HBEs. Considering the square itself, the two sub-spaces on the bottom of this outdoor space are protected by the direct floodwater thanks to the building placed along it. Thus, their  $DV_i$  refer to low risk for stability conditions, as shown by the green sub-spaces of the square of *Scenario 2.C* in Figure 4-A. Meanwhile, the two sub-spaces on the top of the square are directly hit by floodwaters, thus causing extreme risk conditions for stability, as shown by the red sub-spaces of the square of *Scenario 2.C* in Figure 4-A.

In view of these microscale results, Figure 4-A also outlines the position of gathering areas in the two considered evacuation strategies. As shown by the arrow signs in Figure 4-A, the positions of the gathering areas in “leaving” strategy are considered at the downstream exits of the HBE streets, regardless of the  $DV_i$  conditions. On the contrary, as shown by the magenta dots in Figure 4-A, the position of the gathering areas in “sheltering” strategies is different in each analysed scenario because the layout influences  $DV_i$ . They are placed in outdoor spaces and sub-spaces characterized by lower  $DV_i$ , as discussed above, so as to allow pedestrians to wait for the rescuers’ arrival in safer conditions in terms of stability.

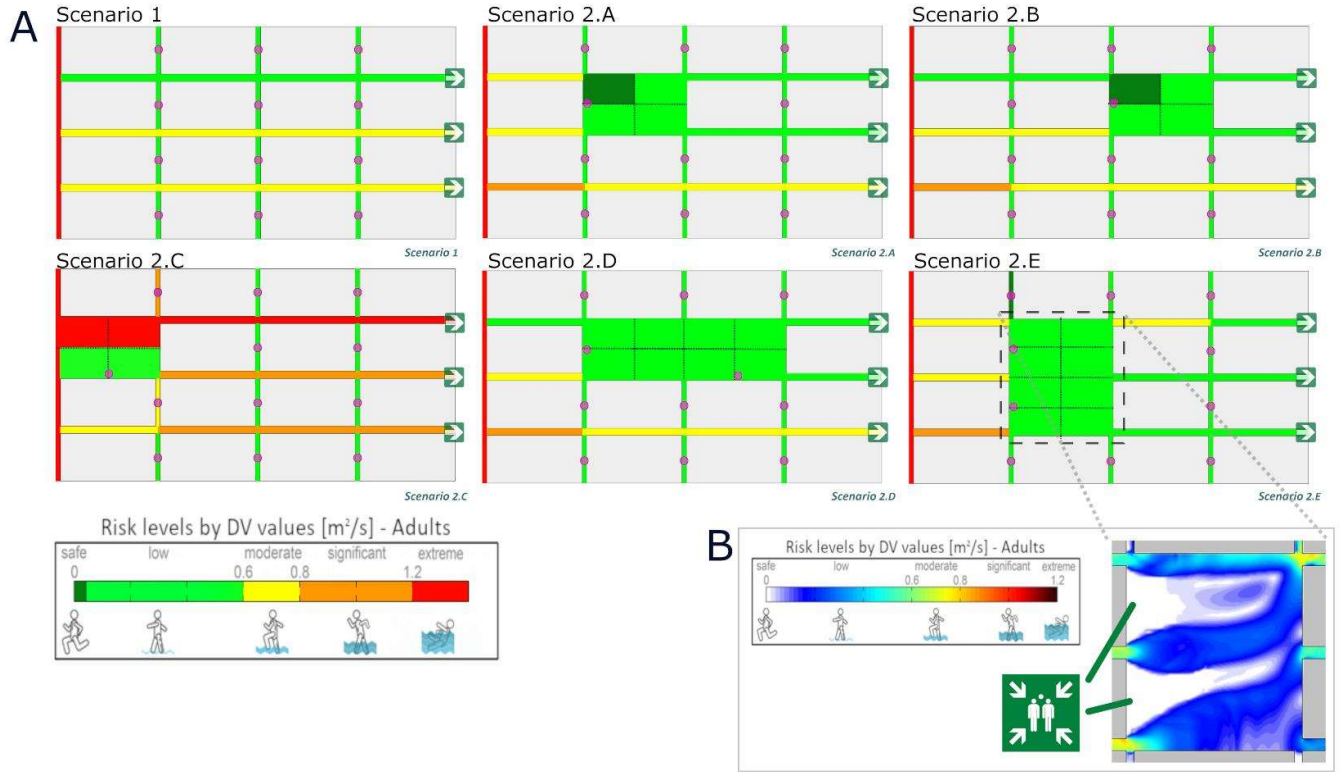


Figure 4:  $DV_i$  maps for each typical HBE, in respect to adopted stability limits conditions (Cox et al., 2010), by offering: A) the conditions of each outdoor spaces and sub-spaces (i.e. for squares, see the dotted lines) and the localization of gathering areas in "sheltering" (magenta dots) and "leaving" (arrow signs) evacuation strategies; B) an example (Scenario 2.E) of local  $DV$  conditions in the main square according to the  $1\text{m} \times 1\text{m}$  solving mesh, by including the gathering areas posing according to the "sheltering" strategy. For each panel, the scale representation of  $DV$  values is offered.

From a macroscale standpoint, Table 6 summarizes the values  $DV_{a,M}$  and  $I_{DV,M}$  (that is equal to  $RI_{HBE,M}$ ). Results show that the typical HBEs in the Scenarios 2 are generally characterized by lower  $DV_{a,M}$  values in comparison to the Scenario 1. As a consequence, the microscale effects of the floodwater spreading into the outdoor spaces in the HBE are confirmed. Nevertheless, as pointed out above, the Scenario 2.C shows the highest risk level from a macroscopic standpoint because of the square position in the aligned layout. Furthermore, typical HBEs with wider squares not just behind the river, that are Scenarios 2.D and 2.E, seem to be less risky than the others, thanking the possibility of a positive impact of such "detention" basins. No significant difference emerges by changing the direction of the major axis.

Typical HBE	$DV_{a,M} [-]$	$I_{DV,M} = RI_{HBE,M} [-]$
Scenario 1	0.65	0.54
Scenario 2.A	0.49	0.41
Scenario 2.B	0.50	0.42
Scenario 2.C	0.98	0.82
Scenario 2.D	0.42	0.35
Scenario 2.E	0.41	0.34

Table 6:  $DV_{a,M}$  and  $I_{DV,M}$  values for each typical HBE as graphically described in Figure 2.

### 3.3. HBE flood risk **with and without** the pedestrian evacuation behaviours

Table 7 summarizes the KPI and  $RI$  values for the typical HBEs, **with and without** the *pedestrian evacuation behaviours*, and by including the specific evacuation strategies, according to the macroscale standpoint.

Evacuation simulation results are reported in Appendix C.

In general terms, the effects of accounting or not the *pedestrians evacuation behaviours* have no relevant effects at the macroscale, as shown by Table 7. In fact, higher  $RI_{HBE,M}$  values correspond to higher  $RI_{evac,M}$  values, essentially because of the impact of  $I_{DV,M}$  on both the risk indexes. Nevertheless,  $RI_{evac,M}$  varies depending on the evacuation management strategies and the last column of Table 7 highlights how the “*sheltering*” strategy always decreases the risk. Considering the KPIs based on the *pedestrian evacuation behaviours*, the *Scenario 2.C* highlights the most critical risk conditions in both the emergency management strategies. The main impact is due to  $T_{e,M}$  and  $N_{a,M}$ , which consider how pedestrians can be trapped during the evacuation process, essentially because of their position with respect to the square. In fact, in *Scenario 2.C*, trapped pedestrians are initially pedestrians placed upstream and near to the square, thus suffering higher  $DV$  levels that both: (1) slow down their motion, as shown by  $T_{e,M}$ ; and (2) can provoke the loss of stability, as shown by  $N_{a,M}$ .

TYPICAL HBE		KEY PERFORMANCE INDICATORS					RISK INDEX		$RI_{evac,M}$ Reduction [%]
Scenario	Strategy	$T_{e,M}$ [-]	$D_{t,M}$ [-]	$N_{a,M}$ [-]	$F_{e,M}$ [-]	$I_{DV,M}$ [-]	$RI_{HBE,M}$	$RI_{evac,M}$	
1	Leaving	<b>0.38</b>	1.00	0.00	0.75	0.54	<b>0.54</b>	<b>0.45</b>	-
	Sheltering	<b>0.11</b>	0.30	0.00	0.15	0.54	<b>0.54</b>	<b>0.34</b>	-24%
2.A	Leaving	<b>0.36</b>	1.00	0.00	0.73	0.41	<b>0.41</b>	<b>0.39</b>	-
	Sheltering	<b>0.11</b>	0.30	0.00	0.07	0.41	<b>0.41</b>	<b>0.26</b>	-33%
2.B	Leaving	<b>0.37</b>	0.99	0.00	0.73	0.42	<b>0.42</b>	<b>0.39</b>	-
	Sheltering	<b>0.11</b>	0.29	0.00	0.07	0.42	<b>0.42</b>	<b>0.27</b>	-33%
2.C	Leaving	<b>1.00</b>	0.95	0.65	0.91	0.82	<b>0.82</b>	<b>0.76</b>	-
	Sheltering	<b>1.00</b>	0.30	0.39	0.50	0.82	<b>0.82</b>	<b>0.59</b>	-21%
2.D	Leaving	<b>0.34</b>	0.99	0.00	0.71	0.35	<b>0.35</b>	<b>0.37</b>	-
	Sheltering	<b>0.11</b>	0.29	0.00	0.00	0.35	<b>0.35</b>	<b>0.23</b>	-38%
2.E	Leaving	<b>0.35</b>	0.99	0.00	0.69	0.34	<b>0.34</b>	<b>0.36</b>	-
	Sheltering	<b>0.11</b>	0.30	0.00	0.06	0.34	<b>0.34</b>	<b>0.22</b>	-39%

Table 7: summary of the KPIs and risk indexes values **with** ( $RI_{evac,M}$ ) **and without** ( $RI_{HBE,M}$ ) pedestrian evacuation behaviours, and depending on the evacuation management strategies. The  $RI_{evac,M}$  Reduction is calculated in percentage terms with respect to the  $RI_{evac,M}$  in “leaving” strategy.

The microscale standpoint confirms the same trends. For each outdoor space and sub-space, Figure 5 and Figure 6 resume  $RI_{HBE,m}$  (panel A) and  $RI_{evac,m}$  (panel B for “leaving” and panel C for “sheltering”).  $RI_{HBE,m}$ -related maps do not change with the evacuation strategy, since the index is based on KPIs representing the HBE geometry and morphology through  $D_{r,m}$  and the event’s magnitude through  $I_{DV,m}$ . On the contrary,  $RI_{evac,m}$



includes the effects of *pedestrian evacuation behaviours* since it includes  $N_{a,m}$  indeed.

According to Figure 5 and Figure 6, apart from *Scenario 2.C*, the squares are characterized by a lower risk than the streets that link them to the river, thanks to the aforementioned “detention basin”-like effect. This result confirms the outcomes of Section 3.2.

The *pedestrian evacuation behaviours* exalt the risks in the squares sub-spaces in which the floodwaters enter from/exit **towards** the linked streets. In view of this phenomenon, streets placed downstream with respect to the **squares**<sup>11</sup> generally present equal or worse conditions than the squares themselves, because they are drain elements for them. **When** trapped pedestrians along these paths are present,  $RI_{evac,m}$  is higher than  $RI_{HBE,m}$  by evidencing the streets where pedestrians could not end the motion process, in view of the abovementioned  $N_{a,m}$  contribution.

On the contrary, the outdoor spaces placed further from the river are characterized by  $RI_{evac,m} < RI_{HBE,m}$  since the simulation results point out how the pedestrians could still move along them and reach a safe area or leave the flood-affected area without additional threats, such as being trapped. This case is reported, for instance, in:

1. the squares of *Scenario 2.B* and *Scenario 2.E*, due to the positive effects of these squares as detection basins;
2. **most** of the perpendicular streets of *Scenario 1*;
3. the perpendicular streets in *Scenario 2.C* in the bottom right part of the HBE, as an effect on pedestrians’ motion due to the lower  $RI_{HBE,m}$  in comparison to the ones closer to the river.

**In** this sense, the sub-space of the square in *Scenario 2.C* offers a valuable difference due to  $N_{a,m}$  in respect to the two proposed strategies, as pointed out by the comparison between Figure 6-B and Figure 6-C.  $RI_{evac,m}$  is lower than  $RI_{HBE,m}$  of about 15% in “leaving”, while of about 30% in “sheltering”.

Finally, in percentage terms, differences between  $RI_{evac,m}$  and  $RI_{HBE,m}$  for the considered spaces vary of about 15% in absolute terms.

---

<sup>11</sup> In this case, higher risks are related to the linked streets having a lower altitude in respect to the upstream part of the square

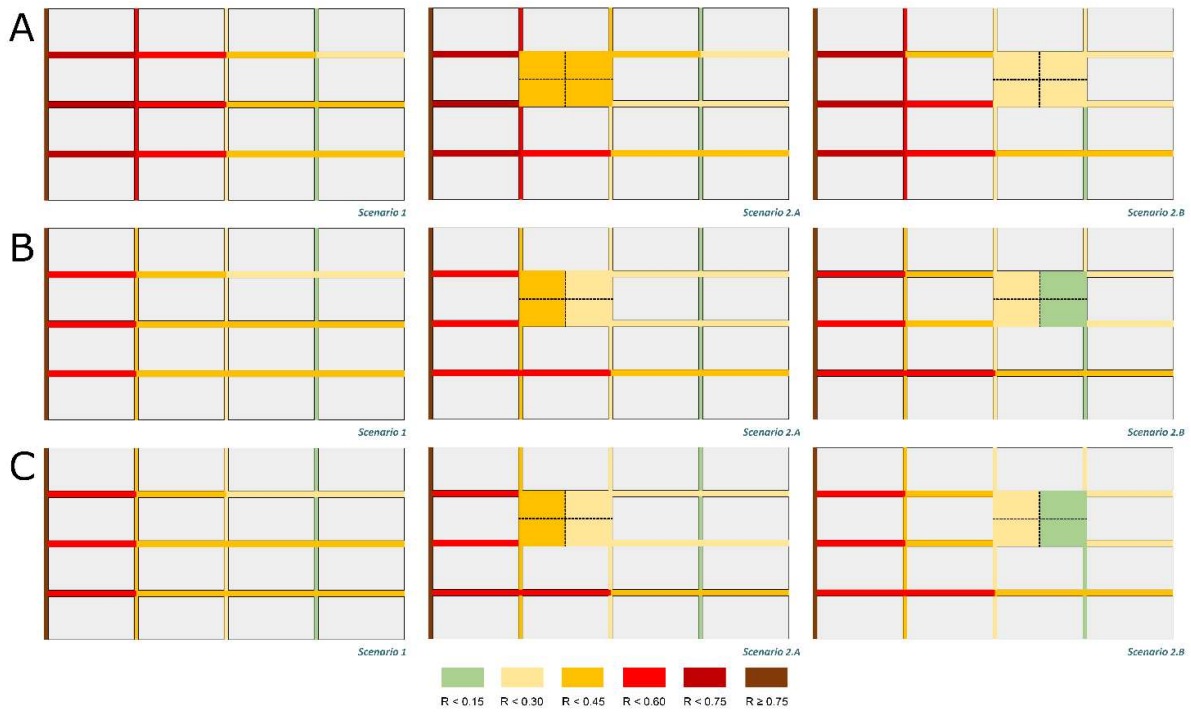


Figure 5: RI maps at the microscale level by considering Scenario 1, 2.A and 2.B: A) without pedestrian evacuation behaviours; B) with pedestrian evacuation behaviours in “leaving” strategy; C) with pedestrian evacuation behaviours in “sheltering” strategy.

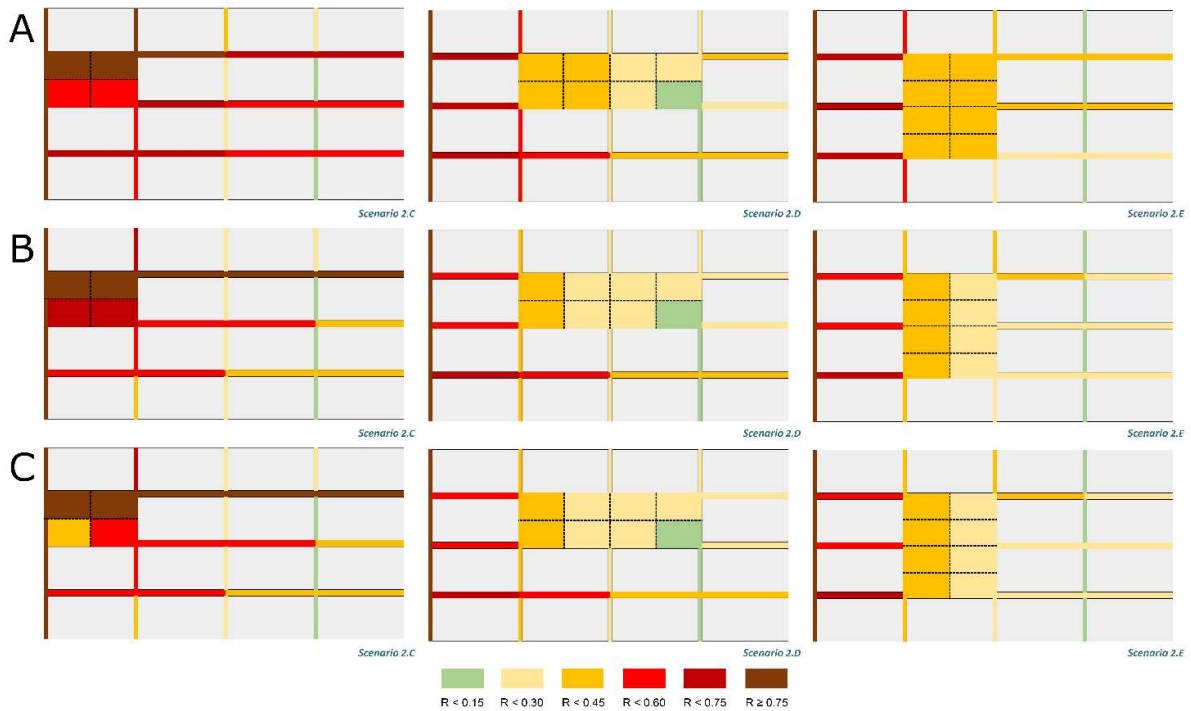


Figure 6: RI maps at the microscale level by considering Scenario 2.C, 2.D and 2.E: A) without pedestrian evacuation behaviours; B) with pedestrian evacuation behaviours in “leaving” strategy; C) with pedestrian evacuation behaviours in “sheltering” strategy.

#### 4. Discussion

##### 4.1. Typical HBE risk comparison

Microscale and macroscale results allow providing some general considerations about the tested typical riverine HBEs, which can be categorized as different variations of an aligned layout configuration. These considerations can be also related to risk assessment *with or without* the *pedestrian evacuation behaviours*, thus demonstrating the capabilities of the novel approach in solving the research assumptions of Section 1. Anyway, it is worth noticing that the following remarks do not want to move towards universal rules regarding the HBE and they are strictly related to the modelled flood and to the considered case studies to define the tested layout. However, they surely represent the first attempt to be done in that direction.

First, regardless of accounting or not *pedestrian evacuation behaviours*, in each typical HBE, the risk levels of the outdoor spaces decrease with the distance from the river. *The* street adjacent to the river is always characterized by the extreme risk level, because of the effects of floodwaters flow entrance due to the river overflow. Considering the assumed time span for the simulations, *DV* conditions do not allow the positioning of gathering areas in these outdoor spaces, while physical retains and supports for evacuation motions (e.g. handrails or raised platforms) can have a limited impact too. These outcomes underline the importance of technological systems to prevent or slow down the river overflow, as well as the importance of early warning systems to improve the safety especially for the HBE areas closer to the river (Cools et al., 2016; La Rosa & Pappalardo, 2020; Wang, 2015).

Considering risk assessment without the *pedestrian evacuation behaviours*, higher risk levels are related to more compact HBEs, such as: (1) *Scenario 1*, where the compact layout forces the floodwater motion towards the downstream exits of the HBE; (2) *Scenario 2.C*, where the presence of a square adjacent to the river may amplify the effects of floodwater spreading in the other outdoor spaces, since the square firstly collects and then pours larger volumes of water towards the linked streets placed downstream.

*Lower* risks are related to the typical HBEs with a non-adjacent square placed. In fact, according to Table 6,  $RI_{HBE,M}$  values in *Scenarios 2.A, 2.B, 2.D* and *2.E* are almost the same (variations lower *than 23%* with respect to minimum  $RI_{HBE,M}$ ). In these cases, *the higher the square dimension, the lower the risk of the spaces*, both from microscale and macroscale standpoints. Furthermore, from a microscale standpoint, the *streets* parallel to the river are characterized by a lower risk than the perpendicular ones, regardless of the typical HBE layout.

1 This result is due to the abovementioned effects of floodwater spreading downstream, that is far from the  
2 river.

3  
4 Although differences **considering** *RI* without *pedestrian evacuation behaviours* exist, similar trends are also  
5  
6 seen for risk assessment with *pedestrian evacuation behaviours*. **The** final outcomes depend on the  
7  
8 considered emergency management strategies. From the macroscale standpoint, in all the considered typical  
9  
10 HBEs, “*sheltering*” seems to be more efficient than “*leaving*”. In fact,  $RI_{evac,M}$  is reduced up to 40%, essentially  
11  
12 because interferences between the pedestrians and the floodwaters are limited in terms of path length and  
13  
14 motion timing. The presence of trapped pedestrians occurs only in *Scenario 2.C*, but their number is lower in  
15  
16 “*sheltering*” strategies in comparison to “*leaving*”.

17  
18  
19  
20  
21 **Reasons** for the improvement under the “*sheltering*” strategies are linked to the microscale *DV* assessment,  
22  
23 that quickly suggests where to place the gathering areas, as shown by Section 3.2. From a general point of  
24  
25 view, it could be considered that gathering areas could be placed along the parallel streets and the upstream  
26  
27 part of the squares, close to the buildings. Such positions can take advantages of the protection from direct  
28  
29 floodwaters impact due to the buildings themselves, as also shown by Figure 4-B and Figure C1 in Appendix  
30  
31 C. In such parts, safety planners could implement signage systems and, eventually, raised platforms where  
32  
33 to gather, so as to avoid further threats over time (Bernardini, Postacchini, et al., 2017; Yamashita et al.,  
34  
35 2016). A widespread implementation of these gathering areas can ensure a reduction of the pedestrians’  
36  
37 threats while moving, because the evacuation path is quite short for each pedestrian.

38  
39  
40  
41  
42 **Anyway**, evacuation simulations can test different quantities of such gathering areas. **Thus**, the optimization  
43  
44 of their number **can be pursued** in respect of their benefits, according to the provided KPIs and *RI* accounting  
45  
46 for *pedestrian evacuation behaviours*.

47  
48  
49 In each typical HBE, simulation outcomes additionally suggest how evacuation systems **support** pedestrians’  
50  
51 motion and stability in floodwater, such as handrails where hanging on (Bernardini, Postacchini, et al., 2017),  
52  
53 should be generally implemented along the streets parallel to the river, especially for those placed nearer to  
54  
55 the river. Along these streets, handrails can be integrated in the building façade as well as by means of **urban**  
56  
57 furniture. Handrails should be also installed in the square of *Scenario 2.C*, so as to help pedestrians in moving  
58  
59  
60  
61  
62  
63  
64  
65

towards the gathering area in the square itself. In the square, such handrails can be included in the urban furniture placed inside the outdoor space itself, being also combined by architecturally-integrated raised platforms. In this sense, heritage preservation issues should be also evaluated from an aesthetic point of view. In view of the above, quick planning of emergency areas could be easily reached for the whole HBE, thus speeding up local authorities and Civil Body Protection actions to this end in a sustainability perspective.

#### 4.2. Key findings, work novelties and future works

Five main issues demonstrate the research key findings, its novelties, and the future works to be carried out by adopting the proposed approach.

First, this work is a first attempt to compare how accounting or not the *pedestrian evacuation behaviours* can affect the flood risk assessment in HBEs. As shown in the results section, differences between  $RI_{HBE,m}$  and  $RI_{evac,m}$  are noticed in all the typical HBEs and can lead to discrepancies in the definition of risk-mitigation strategies for the immediate flood response phase and the evacuation process. In this sense, the proposed approach can support existing methodologies for the assessment of emergency actions and related mobility for the rescuers and the population (Lumbroso & Davison, 2018; Rezende, Miranda, et al., 2019; Shirvani et al., 2020).

Second, according to a sustainability perspective in the methodology application, this work provides an easy-to-use simulation model for evacuation simulation, which is based on a quick setup of commercial generic software. The simulator can be ideally used by low-trained and non-expert technicians, such as the ones of Local Authorities. The model can simulate man-environment interactions at a microscopic level, since the model assigns emergency evacuation rules to each of the simulated agents. Considering previous works on evacuation simulation models and applications (Bernardini, Postacchini, et al., 2017; Lumbroso & Davison, 2018), this approach can:

1. provide a more rapid application of the simulator also in real-world environments, because of the simpler setup of the behavioural and motion quantities in respect to microscopic models;
2. improve the reliability of simulation in respect to simplified macroscopic models, such as the fluid-dynamics ones.

As for the quick evacuation simulation approach, the key performance indicators could support rapid evaluations since they are based on a few simple parameters concerning the simulation outputs. Anyway, it is worth noting that this work considers average and homogeneous *pedestrian evacuation behaviours* and pedestrian features. Some simplifications are hence assumed, including those on neglected factors such as mobility, age and gender, as well as the effective familiarity with the urban layout and the emergency strategies (Lumbroso & Davison, 2018). Future works should try to include such issues. If commercial tools will not be able to quickly include such issues, custom and more complex tools can be used, according to same microscopic evacuation simulation modelling, and without changing the overall evaluation methodology.

Third, the work also innovatively focuses on the outdoor spaces as a key element for flood risk assessment, because of their paramount rule in the evacuation process, thus assessing their impact at their macroscale as well as at the microscale, thus overcoming the general limitations of previous approaches (Lumbroso & Davison, 2018; Shirvani et al., 2020; Zhuo & Han, 2020). In this process, risk assessment with *pedestrian evacuation behaviours* can include or not the impact of emergency evacuation strategies at both the scales, as stated above. The macroscale assessment allows comparing and ranking the risk of a specific HBE. The microscale assessment allows comparing the risk into specific parts of the outdoor space in the HBE, with the final aim at providing data on where and how to introduce interventions for risk mitigation and support pedestrians in emergency conditions.

Fourth, in view of the previous novelty, this work is one of the first attempts in comparing the effectiveness of emergency management strategies based on “leaving” the flood-affected area and on “sheltering” inside it. Furthermore, this comparison has been not provided by previous works, that generally focus on simple evacuation strategies organizations, such as gathering on safe areas or move upstairs in buildings (Lumbroso & Davison, 2018). In this perspective, future efforts should investigate possible variations in each of these strategies, by both investigating the effects in the quantities of evacuation paths and gathering areas and the combination between these strategies indeed.

Finally, this work is oriented towards HBE contexts. The paper proposes a first simulation-based methodology

that tries to provide a parametric characterization of the HBE. In particular, it defines typical scenarios based on a statistical analysis of the main geometrical parameters describing real-world HBEs prone to floods effects. To this aim, relevant real-world HBEs are selected basing on the recurring features in the Italian contexts and by considering urban scenarios already subject to flood. Then, according to the research focus on the outdoor spaces, the combined macroscale and microscale assessment approach innovatively allows ranking and comparing: (1) the overall risk for different typical HBEs, giving general results; (2) the risk of each outdoor space inside the same HBE, as well as in different typical HBEs.

In this process, the *pedestrian evacuation behaviours* in flood are also assessed for risk assessment purposes, for the first time. It is clear that the results hold inside the adopted physical parameters and the considered hazard. On the contrary, the methodology can be applied to other HBEs far from such considered ones, as well as in non HBE context, and can also assess the impact of other flood typologies (European Commission, 2015). The simulation results and related risk assessment outcomes can be considered as valid for HBEs having such typical analysed scenarios, as well as non-HBEs having the same features, under the riverine contexts and the overflow of the river. In view of the above, future works will be able to increase the sample of real-world HBEs to enhance the description of typical HBE scenarios, introduce additional physical configurations also with respect to the river features. Meanwhile, additional works will be able to provide further analysis on additional HBE-characterizing factors, such as i.e. the surface description, the vulnerability of buildings in view of flood-induced damages.

## 5. Conclusions

Flood risk in riverine Historic Built Environment (HBE) depends on the correlation between its *physical vulnerability* and the severity and frequency of hazard, as well as on the immediate response of hosted communities, in view of their *exposure* and *pedestrian evacuation behaviours*.

Basing on a behavioural-based simulation methodology, this work demonstrates that accounting or not the *pedestrian evacuation behaviours* in risk assessment could lead to differences in evaluations. According to the proposed risk indexes and considering the HBE scenarios of this work, risk indexes have the same trends at the macroscale level, that is considering the risk for the whole HBE. On the contrary, differences are more

relevant at the microscale level, that is considering each outdoor space composing the HBE, such as squares and streets. **Considering** the risk assessment without *pedestrian evacuation behaviours*, the risk seems to be overestimated in those outdoor spaces where pedestrians can safely move and/or gather indeed, while the risk seems to be underestimated where pedestrians can be trapped because they have not enough time to reach a safe area. At the same time, the magnitude of overestimations/underestimations depends on the specific conditions of the HBE layout, thus remarking the impact of such flood-affecting factor in risk assessment.

In this way, the proposed risk indexes at the microscale level can be organized into risk maps, which are easy-to-apply tools for the support of safety designers, local **authorities**, and Civil Protection Bodies. These stakeholders can identify priority areas for risk-mitigation strategies, arranging suitable and sustainable evacuation management plans and putting in place support systems for the pedestrians (e.g. gathering areas, also hosted by raised platforms; handrails to have support while moving in critical floodwaters). According to this application perspective, the proposed assessment and comparison methodology could be applied to compare: **(1)** different HBE layouts, by varying the *physical vulnerability* modelling; **(2)** different flood events, by varying the *hazard* modelling; **and (3)** different emergency plans, by varying the *exposure* modelling.

Finally, risk indexes **with and without** *pedestrian evacuation behaviours* defined in this work are static ones, **because** they provide a unique value for the whole analysed event. In this sense, further researches should move towards dynamic (time-dependent) indexes, which could be also defined by replicating the proposed methodology at different (discrete) time steps of the flood event. According to this dynamic approach to risk assessment, future works should also take into account the possibility of coupling the effects of early warning systems to evaluate the safety into the HBE over the time.



## Appendix A: case studies general characterization

City	Paved	Area [m <sup>2</sup> ]	Distance from the river [m]	Number of streets linked [-]	Major axis of the square direction
Albenga	Yes	9235	0-100	8	Perpendicular to the river
Carrara	Yes	3510	0-100	6	Perpendicular to the river
Colorno	Yes	4559	0-100	4	Perpendicular to the river
Montevarchi	Yes	1820	200-300	5	Parallel to the river
Senigallia	Yes	1264	100-200	6	Parallel to the river

Table A.1: Main features of the squares in the case studies.

River - City	River basin area [km <sup>2</sup> ]	River length [km]	Maximum section width [m] (**)
Centa River – Albenga	432.0	45.0	95.0
Carrione River – Carrara	46.6	15.4	10.0
Parma Creek - Colorno	618.0 (*)	-	50.0
Dogana Creek - Montevarchi	27.8	-	15.0
Misa River - Senigallia	380.0	48.0	35.0
STUDY CASE: Esino a Moie Station	801.7	71.4	56.0
(*) this value refers to the closing section of the Ponte Bottego station, Parma (16 km upstream to Colorno); (**) evaluated in proximity of the city centre.			

Table A.2: Main features of the river basin in the considered case studies, by comparing them with the river used for hazard modelling.

## Appendix B: Hazard modelling: hydrograph calculation

The hydrodynamic simulation is based on the flood event registered in 18/11/1975 at Moie (AN) station in the Esino River, whose *maximum measured flow rate* was  $Q_{MEAS} = 442 \text{ m}^3/\text{s}$ , as shown in Figure B1 (grey line).

This event has been introduced in the hazard modelling for the HBE scenarios, by deriving the *maximum flow rate of the studied river cross-section*  $Q_{SECTION} [\text{m}^3/\text{s}]$  as in Eq. B.1:

$$Q_{SECTION} = k_s A R_h^{2/3} \sqrt{i} \quad \text{Eq. B.1}$$

In which:

- $k_s [\text{m}^{1/3}/\text{s}]$  is the Strickler hydraulic roughness due to the riverbed material, assumed equal to  $33 \text{ m}^{1/3}/\text{s}$ ;
- $A [\text{m}^2]$  is the cross-sectional area of flow;
- $R_h [\text{m}]$  is the hydraulic radius, which is the cross-sectional area of flow divided by the wetted perimeter;
- $i [\%]$  is the riverbed slope, which is equal to 0.3%.

Since  $Q_{SECTION}$  ( $566 \text{ m}^3/\text{s}$ ) resulted higher than  $Q_{MEAS}$  ( $442 \text{ m}^3/\text{s}$ ), this configuration could not imply any floods in the given area. To this end, a new flood hydrograph is obtained by multiplying the original one (relating to

$Q_{MEAS}$ ) with an amplification factor equal to 2.5. As shown by Table B1, applying the theory of Giandotti (Giandotti, 1934), we obtain a 100-yr maximum flow rate of 1148 m<sup>3</sup>/s, which is consistent with previous estimations for the case study (VV.AA., 2005). The Moie river gauge was operative until 1978 and, until now, no event with a comparable peak flow-rate was measured.

Return Time	20 years	50 years	100 years	200 years	300 years	500 years
Q [m <sup>3</sup> /s]	894	1039	<b>1148</b>	1256	1320	1399

Table B1: flow rate values for different return times for Esino river, Moie section.

Due to the excessive duration of the time of concentration (18 hours), the final hydrograph has been modified by considering a time of concentration of 6 hours. This choice allows reducing the time span able to influence the evacuation process by inducing critical motion conditions for pedestrians. In this way, the overflow determined by the flood event is condensed in three hours, with almost an hour necessary to reach the maximum flow rate from its beginning. Figure B1 compares the flood hydrographs for the aforementioned considered conditions, by showing the one adopted in HBE-related simulations by the red curve.

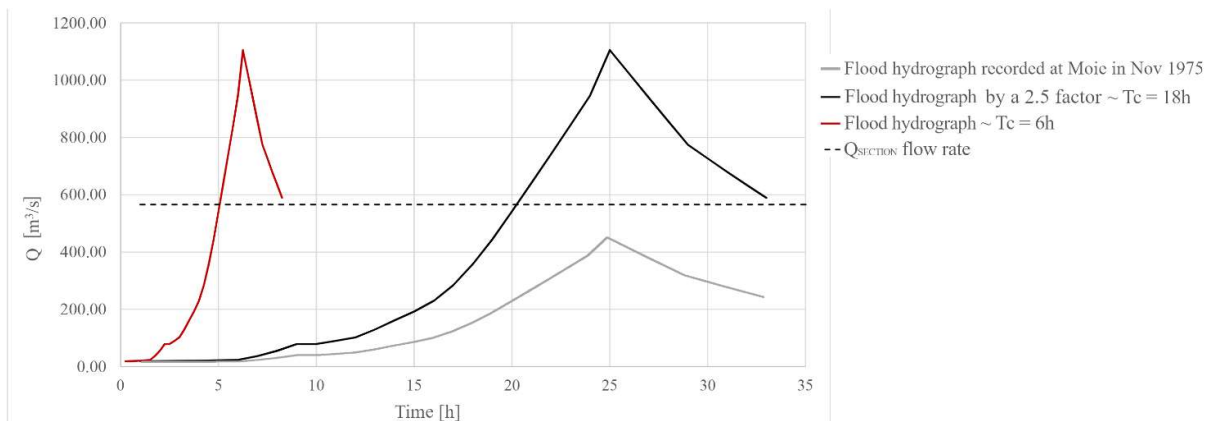


Figure B1. Flood hydrographs comparison in respect to  $Q_{SECTION}$  (dashed line): measured data, by the grey curve (VV.AA., 2005), data incremented by a 2.5 factor (concentration of 18 hours), by the black curve, data used in the HBE simulation (concentration of 6 hours), by the red line.

## Appendix C: Simulation results

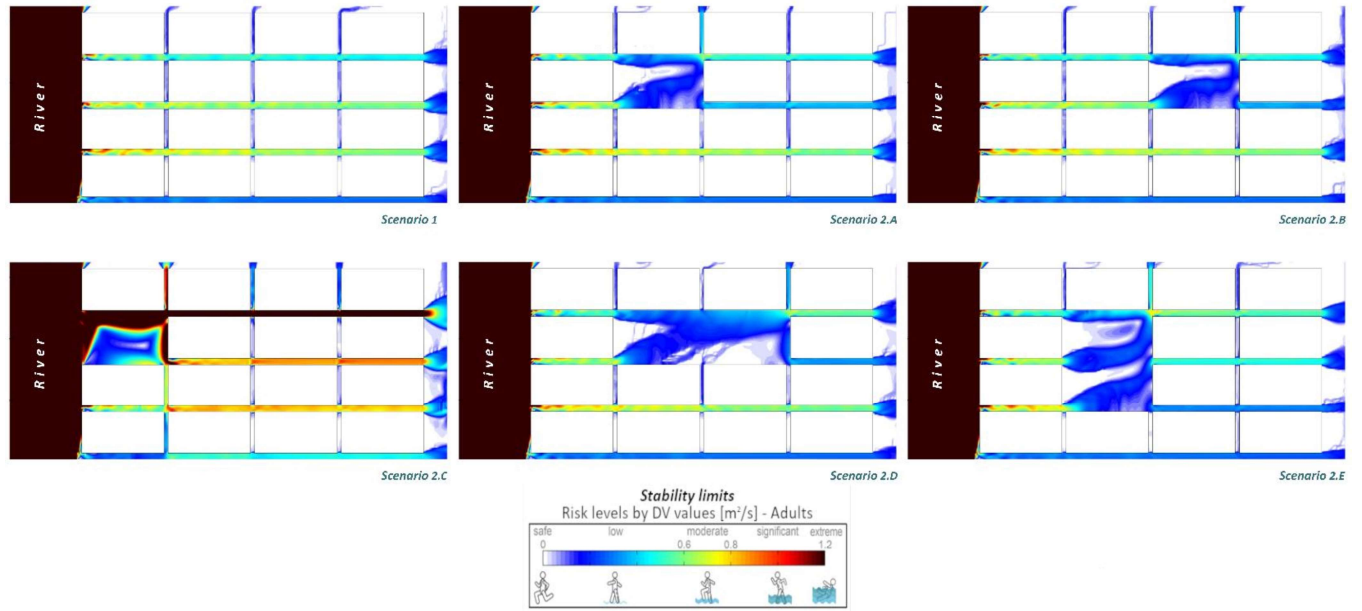


Figure C1. Local DV conditions in the outdoor spaces for each typical HBE, affecting stability. Data are shown according to the 1m x 1m solving mesh, by including the continuous scale representation of DV values (on the bottom).

STUDY CASE		OUTPUTS			
Scenario	Strategy	$t_{\max, \text{evac}}$ [s]	$d_{\max}$ [m]	$n_a$ [pp]	$f_{e95}$ [pp/s]
1	Leaving	460	278.37	0	0.53
	Sheltering	131	82.56	0	1.82
2.A	Leaving	436	277.85	0	0.57
	Sheltering	128	82.44	0	1.98
2.B	Leaving	440	276.43	0	0.57
	Sheltering	128	80.59	0	1.98
2.C	Leaving	1200	265.79	156	0.18
	Sheltering	1200	82.45	93	1.07
2.D	Leaving	413	276.44	0	0.62
	Sheltering	127	79.95	0	2.14
2.E	Leaving	422	276.26	0	0.67
	Sheltering	126	83.88	0	2.00

Table C.1: results from evacuation simulations.

## Appendix D: Notations

Notation	Unit of measure	Macroscopic (M) or microscopic (m)	Definition
$A_i$	[m <sup>2</sup> ]	m	area of a specific outdoor space $i$
$b$	[m]	n.a.	parallel (with respect to the river) base of the building blocks based on a rectangular shape representation and perpendicular length $l$ [m]
$D$	[m]	n.a.	floodwater depth
$d_{\max}$	[m]	M	longest evacuation path according to the evacuation simulation results
$d_r, d_{r, \text{MAX}}$	[m]	m	the Euclidean distance between the river axis and the barycenter of the outdoor space or sub-space, and related maximum value considering the outdoor spaces in the HBE
$D_{r, m}$	[-]	m	normalized distance from the outdoor space to the river
$D_{t, M}$	[-]	M	normalized travelled distance based on the evacuation simulation

			results
DV	[m <sup>2</sup> /s]	n.a.	multiplication between the floodwater depth D and speed V
DV <sub>a,M</sub>	[m <sup>2</sup> /s]	M	average DV value weighted by the outdoor space areas
DV <sub>i</sub>	[m <sup>2</sup> /s]	m	DV value suffered by the pedestrians in the considered outdoor space <i>i</i>
DV <sub>max,i</sub>	[m <sup>2</sup> /s]	M	maximum value of DV during the simulation time, for all the outdoor spaces <i>i</i>
f <sub>e95</sub> , f <sub>e95,MAX</sub>	[pp/s]	M	pedestrian flow at the gathering areas calculated considering the 5 <sup>th</sup> to 95 <sup>th</sup> percentiles of pedestrians, and related maximum value
F <sub>e,M</sub>	[-]	M	normalized pedestrian flow based on the evacuation simulation results
HBE	acr	acr	Historic Built Environment
I <sub>DV,M</sub>	[-]	M	stability index for the whole HBE
I <sub>DV,m</sub>	[-]	m	stability index for each outdoor area
l	[m]	n.a.	perpendicular (with respect to the river) length of the building blocks based on a rectangular shape representation
KPI	acr	acr	Key Performance Indicator
M	[m <sup>3</sup> /m]	m	floodwater flow specific force for width unit
n <sub>a</sub>	[pp]	M	number of pedestrians unable to arrive in a gathering area
N <sub>a,M</sub>	[-]	M	percentage of non-arrived pedestrians based on the evacuation simulation results
N <sub>a,m</sub>	[Boolean]	m	presence of trapped pedestrians in a given outdoor space based on the evacuation simulation results
P	[pp]	M	whole number of simulated pedestrians
RI	[-]	n.a.	generic Risk Index
RI <sub>evac,M</sub>	[-]	M	macroscale RI without pedestrian evacuation behaviours
RI <sub>evac,m</sub>	[-]	m	microscale RI without pedestrian evacuation behaviours
RI <sub>HBE,M</sub>	[-]	M	macroscale RI with pedestrian evacuation behaviours
RI <sub>HBE,m</sub>	[-]	m	microscale RI with pedestrian evacuation behaviours
T <sub>e,M</sub>	[-]	M	normalized evacuation time based on the evacuation simulation results
t <sub>max,evac</sub>	[s]	M	maximum evacuation time according to the evacuation simulation results
t <sub>sim</sub>	[s]	M	overall simulation time
V	[m/s]	n.a.	floodwater speed
V <sub>p</sub> , V <sub>pi</sub>	[m/s]	m	general pedestrian evacuation speed, and speed depending on DV <sub>i</sub>
w <sub>k</sub>	[-]	n.a.	weight of each parameter in RI calculation according to the Analytical Hierarchy Process

Table D.1: list of symbols and Acronyms used in the main text of this work, including the application to macroscopic or microscopic assessment purposes. "acr" is used for acronyms while "n.a." in the macroscopic/microscopic column implies that no assignment can be done to the variable.

## BIBLIOGRAPHY:

- Arrighi, C., Brugioni, M., Castelli, F., Franceschini, S., & Mazzanti, B. (2013). Urban micro-scale flood risk estimation with parsimonious hydraulic modelling and census data. *Natural Hazards and Earth System Science*, 13(5), 1375–1391. <https://doi.org/10.5194/nhess-13-1375-2013>
- Arrighi, C., Pregnotato, M., Dawson, R. J., & Castelli, F. (2019). Preparedness against mobility disruption by floods. *Science of The Total Environment*, 654, 1010–1022. <https://doi.org/10.1016/j.scitotenv.2018.11.191>
- Baky, M. A. Al, Islam, M., & Paul, S. (2020). Flood Hazard, Vulnerability and Risk Assessment for Different Land Use Classes Using a Flow Model. *Earth Systems and Environment*, 4(1), 225–244. <https://doi.org/10.1007/s41748-019-00141-w>
- Balica, S. F., Popescu, I., Beevers, L., & Wright, N. G. (2013). Parametric and physically based modelling techniques for flood risk and vulnerability assessment: A comparison. *Environmental Modelling & Software*, 41, 84–92. <https://doi.org/10.1016/j.envsoft.2012.11.002>
- Bazin, P.-H., Mignot, E., & Paquier, A. (2017). Computing flooding of crossroads with obstacles using a 2D numerical model. *Journal of Hydraulic Research*, 55(1), 72–84.

<https://doi.org/10.1080/00221686.2016.1217947>

- Beretta, R., Ravazzani, G., Maiorano, C., & Mancini, M. (2018). Simulating the Influence of Buildings on Flood Inundation in Urban Areas. *Geosciences*, 8(2), 77. <https://doi.org/10.3390/geosciences8020077>
- Bernardini, G., Camilli, S., Quagliarini, E., & D'Orazio, M. (2017). Flooding risk in existing urban environment: from human behavioral patterns to a microscopic simulation model. *Energy Procedia*, 134, 131–140. <https://doi.org/10.1016/j.egypro.2017.09.549>
- Bernardini, G., Postacchini, M., Quagliarini, E., Brocchini, M., Cianca, C., & D'Orazio, M. (2017). A preliminary combined simulation tool for the risk assessment of pedestrians' flood-induced evacuation. *Environmental Modelling & Software*, 96, 14–29. <https://doi.org/10.1016/j.envsoft.2017.06.007>
- Bernardini, G., Quagliarini, E., & D'Orazio, M. (2019). Investigating Exposure in Historical Scenarios: How People Behave in Fires, Earthquakes and Floods. In A. Aguilar (Ed.), *Structural Analysis of Historical Constructions - RILEM bookseries* (1st ed., Vol. 18, pp. 1138–1151). Aguilar, R. Torrealva, D. Moreira, S. Pando, M.A. Ramos, L.F. [https://doi.org/10.1007/978-3-319-99441-3\\_123](https://doi.org/10.1007/978-3-319-99441-3_123)
- Bernardini, G., Quagliarini, E., D'Orazio, M., & Brocchini, M. (2020). Towards the simulation of flood evacuation in urban scenarios: Experiments to estimate human motion speed in floodwaters. *Safety Science*, 123, 104563. <https://doi.org/10.1016/j.ssci.2019.104563>
- Bloomberg, M., & Burden, A. (2006). *New York City Pedestrian Level of Service Study—Phase 1*. <http://scholar.google.com/scholar?hl=en&btnG=Search&q=intitle:New+York+City.+Pedestrian+Level+of+Service+Study+Phase+I#1>
- British Standards Institution. (2004). *The application of fire safety engineering principles to fire safety design of buildings-Part 6: Human factors: Life safety strategies — Occupant evacuation, behaviour and condition (Sub-system 6)* (Issue PD 7974-6:2004).
- Chanson, H., & Brown, R. (2015). New criterion for the stability of a human body in floodwaters. *Journal of Hydraulic Research*, 53(4), 540–541. <https://doi.org/10.1080/00221686.2015.1054321>
- Chow, V. T. (1959). *Open-Channel Hydraulics*. Ven Te Chow. McGraw-Hill, New York, 1959. xviii + 680 pp. Illus. \$17. In *Science*.
- Cools, J., Innocenti, D., & O'Brien, S. (2016). Lessons from flood early warning systems. *Environmental Science & Policy*, 58, 117–122. <https://doi.org/10.1016/j.envsci.2016.01.006>
- Cox, R. J., Shand, T. D., & Blacka, M. J. (2010). *Appropriate Safety Criteria for People in Floods - WRL Research Report 240*.
- D'Orazio, M., Longhi, S., Olivetti, P., & Bernardini, G. (2015). Design and experimental evaluation of an interactive system for pre-movement time reduction in case of fire. *Automation in Construction*, 52, 16–28. <https://doi.org/10.1016/j.autcon.2015.02.015>
- De Sousa, N. M., Soares, W. D. A., Da Silva, S. R., & Do Nascimento, E. C. (2019). Contribution of public squares to the reduction of urban flooding risk. *Revista Ambiente e Agua*. <https://doi.org/10.4136/ambi-agua.2374>
- European Commission. (2015). *European Overview Assessment of Member States' reports on Preliminary Flood Risk Assessment and Identification of Areas of Potentially Significant Flood Risk*. <https://doi.org/10.2779/576456>
- European Commission. (2017). Overview of natural and man-made disaster risks in the European Union may face. In *Commission Staff Working Document*. <https://doi.org/10.2795/861482>
- Ferreira, T. M., & Santos, P. P. (2020). An Integrated Approach for Assessing Flood Risk in Historic City Centres. *Water*, 12(6), 1648. <https://doi.org/10.3390/w12061648>
- Gandini, A., Garmendia, L., Prieto, I., Álvarez, I., & San-José, J. T. (2020). A holistic and multi-stakeholder methodology for vulnerability assessment of cities to flooding and extreme precipitation events. *Sustainable Cities and Society*. <https://doi.org/10.1016/j.scs.2020.102437>
- Giandotti, M. (1934). Previsione delle piene e delle magre dei corsi d'acqua (in Italian - Forecast of floods and low levels of watercourses). *Istituto Poligrafico Dello Stato*, 8, 107–117.
- Gu, D. (2019). *Exposure and vulnerability to natural disasters for world's cities*. United Nations, Department of Economics and Social Affairs, Population Division, Technical Paper No. 4. (Population Division, Technical Paper No. 4., Issue Technical Paper No. 4.).

- <https://www.un.org/en/development/desa/population/publications/pdf/technical/TP2019-4.pdf>
- Haq, T., Halik, G., & Hidayah, E. (2020). Flood routing model using integration of Delft3D and GIS (case study: Tanggul watershed, Jember). *AIP Conference Proceedings*, 2278(October), 020052. <https://doi.org/10.1063/5.0014607>
- Hassaballah, K., Mohamed, Y., Omer, A., & Uhlenbrook, S. (2020). Modelling the Inundation and Morphology of the Seasonally Flooded Mayas Wetlands in the Dinder National Park-Sudan. *Environmental Processes*, 7(3), 723–747. <https://doi.org/10.1007/s40710-020-00444-5>
- Kobes, M., Helsloot, I., de Vries, B., & Post, J. G. (2010). Building safety and human behaviour in fire: A literature review. *Fire Safety Journal*, 45(1), 1–11. <https://doi.org/10.1016/j.firesaf.2009.08.005>
- Kolen, B., & van Gelder, P. H. A. J. M. (2018). Risk-Based Decision-Making for Evacuation in Case of Imminent Threat of Flooding. *Water*, 10(10), 1429. <https://doi.org/10.3390/w10101429>
- Kontokosta, C. E., & Malik, A. (2018). The Resilience to Emergencies and Disasters Index: Applying big data to benchmark and validate neighborhood resilience capacity. *Sustainable Cities and Society*, 36(October 2017), 272–285. <https://doi.org/10.1016/j.scs.2017.10.025>
- Kramer, M., Terheiden, K., & Wieprecht, S. (2016). Safety criteria for the trafficability of inundated roads in urban floodings. *International Journal of Disaster Risk Reduction*, 17, 77–84. <https://doi.org/10.1016/j.ijdrr.2016.04.003>
- La Rosa, D., & Pappalardo, V. (2020). Planning for spatial equity - A performance based approach for sustainable urban drainage systems. *Sustainable Cities and Society*, 53, 101885. <https://doi.org/10.1016/j.scs.2019.101885>
- Lanza, S. G. (2003). Flood hazard threat on cultural heritage in the town of Genoa (Italy). *Journal of Cultural Heritage*. [https://doi.org/10.1016/S1296-2074\(03\)00042-6](https://doi.org/10.1016/S1296-2074(03)00042-6)
- Lin, J., Zhu, R., Li, N., & Becerik-Gerber, B. (2020). How occupants respond to building emergencies: A systematic review of behavioral characteristics and behavioral theories. *Safety Science*, 122, 104540. <https://doi.org/10.1016/j.ssci.2019.104540>
- Lumbroso, D., & Davison, M. (2018). Use of an agent-based model and Monte Carlo analysis to estimate the effectiveness of emergency management interventions to reduce loss of life during extreme floods. *Journal of Flood Risk Management*, 11, S419–S433. <https://doi.org/10.1111/jfr3.12230>
- MassMotion Guide. (2017). *MassMotion Guide*. <https://www.oasys-software.com/wp-content/uploads/2017/12/MassMotion.pdf>
- Melo, R., Zêzere, J. L., Oliveira, S. C., Garcia, R. A. C., Oliveira, S., Pereira, S., Piedade, A., Santos, P. P., & van Asch, T. W. J. (2020). Defining evacuation travel times and safety areas in a debris flow hazard scenario. *Science of The Total Environment*, 712, 136452. <https://doi.org/10.1016/j.scitotenv.2019.136452>
- Mogollón, B., Frimpong, E. A., Hoegh, A. B., & Angermeier, P. L. (2016). An empirical assessment of which inland floods can be managed. *Journal of Environmental Management*, 167, 38–48. <https://doi.org/10.1016/j.jenvman.2015.10.044>
- Nguyen, H. Q., Radhakrishnan, M., Bui, T. K. N., Tran, D. D., Ho, L. P., Tong, V. T., Huynh, L. T. P., Chau, N. X. Q., Ngo, T. T. T., Pathirana, A., & Ho, H. L. (2019). Evaluation of retrofitting responses to urban flood risk in Ho Chi Minh City using the Motivation and Ability (MOTA) framework. *Sustainable Cities and Society*, 47, 101465. <https://doi.org/10.1016/j.scs.2019.101465>
- Oppen, S., Cinque, P., & Davies, B. (2010). Timeline modelling of flood evacuation operations. *Procedia Engineering*, 3, 175–187. <https://doi.org/10.1016/j.proeng.2010.07.017>
- Ortiz, R., Ortiz, P., Martín, J. M., & Vázquez, M. A. (2016). A new approach to the assessment of flooding and dampness hazards in cultural heritage, applied to the historic centre of Seville (Spain). *Science of the Total Environment*. <https://doi.org/10.1016/j.scitotenv.2016.01.207>
- Rezende, O. M., Guimarães, L. F., Miranda, F. M., Haddad, A. N., & Miguez, M. G. (2019). A time-integrated index for flood risk to resistance capacity. *Water (Switzerland)*. <https://doi.org/10.3390/w11071321>
- Rezende, O. M., Miranda, F. M., Haddad, A. N., & Miguez, M. G. (2019). A Framework to Evaluate Urban Flood Resilience of Design Alternatives for Flood Defence Considering Future Adverse Scenarios. *Water*, 11(7), 1485. <https://doi.org/10.3390/w11071485>
- Saaty, T. L. (1980). The analytic hierarchy process: planning. *Priority Setting. Resource Allocation*, MacGraw-

Hill, New York International Book Company.

- Sandbach, S. D., Nicholas, A. P., Ashworth, P. J., Best, J. L., Keevil, C. E., Parsons, D. R., Prokocki, E. W., & Simpson, C. J. (2018). Hydrodynamic modelling of tidal-fluvial flows in a large river estuary. *Estuarine, Coastal and Shelf Science*, 212(June), 176–188. <https://doi.org/10.1016/j.ecss.2018.06.023>
- Schadschneider, A., Klingsch, W., Klüpfel, H., Kretz, T., Rogsch, C., & Seyfried, A. (2009). Evacuation Dynamics: Empirical Results, Modeling and Applications. In Meyers R. (Ed.), *Encyclopedia of Complexity and Systems Science* (pp. 3142-3176 LA-English). Springer New York. [https://doi.org/10.1007/978-0-387-30440-3\\_187](https://doi.org/10.1007/978-0-387-30440-3_187)
- Shirvani, M., Kesserwani, G., & Richmond, P. (2020). Agent-based modelling of pedestrian responses during flood emergency: mobility behavioural rules and implications for flood risk analysis. *Journal of Hydroinformatics*, 22(5), 1078–1092. <https://doi.org/10.2166/hydro.2020.031>
- Soares-Frazão, S., & Zech, Y. (2008). Dam-break flow through an idealised city. *Journal of Hydraulic Research*, 46(5), 648–658. <https://doi.org/10.3826/jhr.2008.3164>
- Testa, G., Zuccalà, D., Alcrudo, F., Mulet, J., & Soares-Frazão, S. (2007). Flash flood flow experiment in a simplified urban district. *Journal of Hydraulic Research*. <https://doi.org/10.1080/00221686.2007.9521831>
- United Nations. (2018). *World Urbanization Prospects*.
- Velickovic, M., Zech, Y., & Soares-Frazão, S. (2017). Steady-flow experiments in urban areas and anisotropic porosity model. *Journal of Hydraulic Research*, 55(1), 85–100. <https://doi.org/10.1080/00221686.2016.1238013>
- Villagràn De León, J. C. (2006). Vulnerability: A conceptual and methodological review. In *Source - studies of the university: research, counsel, education* (Issue 4). <http://collections.unu.edu/eserv/UNU:1871/pdf3904.pdf>
- VV.AA. (2005). *Studi e proposte per la definizione del rischio idraulico e dell'erosione nei bacini idrografici delle aree montane - Parte A: rischio idraulico delle aree montane (in Italian - Studies for defining hydraulic risk and erosion in mountain areas)* (P. Salandin (ed.)). Autorità di Bacino della Regione Marche.
- Wang, J. J. (2015). Flood risk maps to cultural heritage: Measures and process. *Journal of Cultural Heritage*, 16(2), 210–220. <https://doi.org/10.1016/j.culher.2014.03.002>
- Wizor, C., & Mpigi, G. (2020). GEOSPATIAL MAPPING OF URBAN FLOOD-PRONE AREAS IN PORT HARCOURT METROPOLIS: IMPLICATIONS FOR EFFECTIVE URBAN PHYSICAL PLANNING IN NIGERIA. *World Journal of Innovative Research (WJIR)*, 8, 17–25.
- Wood, N., Jones, J., Peters, J., & Richards, K. (2018). Pedestrian evacuation modeling to reduce vehicle use for distant tsunami evacuations in Hawai'i. *International Journal of Disaster Risk Reduction*, 28, 271–283. <https://doi.org/10.1016/j.ijdrr.2018.03.009>
- Yamashita, S., Watanabe, R., & Shimatani, Y. (2016). Smart adaptation activities and measures against urban flood disasters. *Sustainable Cities and Society*, 27, 175–184. <https://doi.org/10.1016/j.scs.2016.06.027>
- Young, A. F., & Jorge Papini, J. A. (2020). How can scenarios on flood disaster risk support urban response? A case study in Campinas Metropolitan Area (São Paulo, Brazil). *Sustainable Cities and Society*, 61, 102253. <https://doi.org/10.1016/j.scs.2020.102253>
- Yuksel, M. E. (2018). Agent-based evacuation modeling with multiple exits using NeuroEvolution of Augmenting Topologies. *Advanced Engineering Informatics*. <https://doi.org/10.1016/j.aei.2017.11.003>
- Zhuo, L., & Han, D. (2020). Agent-based modelling and flood risk management: A compendious literature review. *Journal of Hydrology*, 591, 125600. <https://doi.org/10.1016/j.jhydrol.2020.125600>
- Zlateski, A., Lucesoli, M., Bernardini, G., & Ferreira, T. M. (2020). Integrating human behaviour and building vulnerability for the assessment and mitigation of seismic risk in historic centres: Proposal of a holistic human-centred simulation-based approach. *International Journal of Disaster Risk Reduction*, 43, 101392. <https://doi.org/10.1016/j.ijdrr.2019.101392>